Practical guide for curve fitting in x-ray photoelectron spectroscopy

George H. Major, Neal Fairley, Peter M. A. Sherwood, (iD) Matthew R. Linford, (iD) Jeff Terry, Vincent Fernandez, and (iD) Kateryna Artyushkova

COLLECTIONS

Paper published as part of the special topic on Special Topic Collection: Reproducibility Challenges and Solutions

View Online Export Citation CrossMark

ARTICLES YOU MAY BE INTERESTED IN

Practical guide to the use of backgrounds in quantitative XPS
Journal of Vacuum Science & Technology A **39**, 011201 (2021); https://doi.org/10.1116/6.0000661

Assessment of the frequency and nature of erroneous x-ray photoelectron spectroscopy analyses in the scientific literature
Journal of Vacuum Science & Technology A **38**, 061204 (2020); https://doi.org/10.1116/6.0000685

Practical guides for x-ray photoelectron spectroscopy (XPS): Interpreting the carbon 1s spectrum
Journal of Vacuum Science & Technology A **39**, 013204 (2021); https://doi.org/10.1116/6.0000682

Practical guide for curve fitting in x-ray photoelectron spectroscopy

George H. Major,[1] Neal Fairley,[2] Peter M. A. Sherwood,[3] Matthew R. Linford,[1] Jeff Terry,[4] Vincent Fernandez,[5] and Kateryna Artyushkova[6,a]

AFFILIATIONS

[1]Department of Chemistry and Biochemistry, Brigham Young University, C100 BNSN, Provo, Utah 84602
[2]Casa Software Ltd., Bay House, Teignmouth, United Kingdom
[3]Department of Chemistry, University of Washington, Seattle, Washington 98195
[4]Illinois Institute of Technology, 3101 S. Dearborn St., Chicago, Illinois 60616
[5]CNRS, Institut des Matériaux Jean Rouxel, IMN, Université de Nantes, F-44000 Nantes, France
[6]Physical Electronics, 18725 Lake Drive East, Chanhassen, Minnesota 55317

Note: This paper is part of the Special Topic Collection on Reproducibility Challenges and Solutions.
[a]Electronic mail: kartyushkova@phi.com

ABSTRACT

The use of peak fitting to extract information from x-ray photoelectron spectroscopy (XPS) data is of growing use and importance. Due to increased instrument accessibility and reliability, the use of XPS instrumentation has significantly increased around the world. However, the increased use has not been matched by the expertise of the new users, and the erroneous application of curve fitting has contributed to ambiguity and confusion in parts of the literature. This guide discusses the physics and chemistry involved in generating XPS spectra, describes good practices for peak fitting, and provides examples of appropriate use along with tools for avoiding mistakes.

I. INTRODUCTION

Over the past 30 years, x-ray photoelectron spectroscopy (XPS) has become the most widely used surface analysis tool and has been an essential component of many research studies.[1] Curve fitting has been widely used for more than 50 years for extracting chemical information from the overlapping features in high-resolution XPS spectra.[2] Despite computational advances and higher accessibility of software resources, it has been challenging to develop a chemically and physically meaningful approach to curve fitting. The absence of a distinct theoretical description of XPS fitting has led to the publication of erroneous conclusions about surface chemistry.[2,3] In an ongoing study of XPS data in three high profile journals,[3] it was observed that roughly 70% of the papers using XPS analyzed the data using some type of curve fitting. Furthermore, errors, misconceptions, and bad curve-fitting practices accounted for most of the serious problems in both the measured XPS data and the spectral analysis that were identified in more than 30% of the papers analyzed. This guide is intended to help address this important problem.

Curve fitting, also known as peak fitting,[4] is the process used to extract information from the spectral data for a number of techniques. Although the details of curve fitting depend on the technique in question, the curve fitted spectra generally contain overlapping peaks. Each of these peaks is represented by a function that reflects the physical process involved in generating the original signal. XPS data interpretation and representation range from a rudimentary understanding/extraction of the elements present in a material to advanced peak fitting and background analysis that reveal chemical states and sample morphologies.

In XPS, it is convenient to identify two spectral regions, namely, the core region (electrons with binding energies, BEs, greater than 30 eV) and the valence band region (BE < 30 eV). In the core region, the spectral features arise from photoelectrons generated from core energy levels (atomic orbitals), which are characteristic of the individual atoms in the sample.[5] In contrast, the features in the valence band region arise from photoelectrons generated from energy levels that typically involve the chemical

interactions between the atoms in chemical bonding (the molecular orbitals).[5] The spectral features of both the core and valence regions are sensitive to the chemical environments of the atoms in a sample. In the core region, chemical shifts in the BEs yield a series of typically overlapping peaks when the sample has atoms in different chemical environments, e.g., oxidation states.[6] The resulting data can be analyzed by curve fitting. Curve/peak fitting is often the only way to extract quantitative information from these spectra.

The objective of curve-fitting high-resolution core XPS spectra with a set of component peaks is to separate the photoemission signal originating from distinct elemental or chemical states. Parameters of importance extracted from curve fitting are the photoemission peak BE, full width at half maximum (FWHM), lineshapes, and area. The position of a component peak provides evidence for assigning it to an elemental or chemical environment. The FWHM and peak lineshapes are indicators of the chemical and physical environment of the atom. Photoemission peak lineshapes can vary from simple, narrow, symmetric shapes to complex structures characteristic of the different oxidation states of metals.[5] Quantitative information about the concentrations of the chemical states identified is inferred by measuring the relative area of each component peak, the calculation of which requires the separation of zero energy-loss signals from the inelastically scattered background. The determination of accurate approximations to the background signal is also an integral part of the XPS peak fitting process.

Curve fitting is sometimes misdescribed as being deconvolution.[4] Deconvolution is a different process to curve fitting. Deconvolution is a process that attempts to remove the broadening that results from instrumental factors, separating the "true" spectrum from the observed spectrum. The process results in a new spectrum with the data altered by the deconvolution process. Deconvolution will not be discussed in this paper.

Our goal is to demonstrate useful, practical approaches for analyzing XPS core regions (high-resolution or narrow scans) and what common mistakes should be avoided when curve fitting. Although there are several types of common errors in peak fitting, effective and useful approaches to peak fitting vary somewhat with the analysis objective, the type of sample, and the complexity of the spectrum. Fitting may be used to verify the composition of a pure sample (Sec. V), to separate overlapping peaks for quantitative analysis (Sec. VI B 1), to obtain the relative amounts of each phase from a sample with multiple phases of the same element (Sec. VI B 2), and to examine in great detail the chemical spectrum for an element or phase for comparison with theory. This guide describes multiple complications that can appear with fitting the core region, including multiplet splitting, conduction band interactions, and the use of achromatic X-radiation.

The following sections of the paper highlight important topics for consideration during peak fitting. Section II describes a fundamental approach to peak fitting, while Sec. III describes typical peak fitting errors observed in the literature and offers recommendations to avoid them. Section IV addresses issues to think about before starting to curve fit spectra (instrument setup, adequate data collection, charge correction, lineshapes, and phenomena impacting lineshapes and widths). Section V shows the fitting of poly(ethylene terephthalate) (PET) as an example of fitting a reference spectrum from pure material. Section VI summarizes a variety of tools and information that are critical for avoiding common mistakes in curve fitting. Important useful topics addressed include dealing with overlapping peaks, fitting transition metal spectra, appropriately constraining spin–orbit split peak ratios and energy separation, and others.

II. BASIC APPROACH FOR FITTING XPS SPECTRA

A peak fitting model is defined in terms of *component peaks* and a *background* algorithm. The component peaks are specified using *lineshapes*, which are mathematical functions, and fitting parameters that permit a component peak to vary in a variety of ways, including position, FWHM, area, Lorentzian character, degree of asymmetry, and Gaussian character (The first four of these parameters will apply to all peaks, the latter two in some specific cases.) Sets of component peaks are summed (*sum of all component peaks*) and then added to a background to form an approximation to the original data *envelope*.

The procedure of fitting component peaks to reproduce experimental photoemission spectra utilizes mathematical algorithms to minimize a figure-of-merit as a measure of the closeness of the mathematic model to the experimental data. The fitting algorithm incrementally alters the adjustable parameters, which leads from a current state to a termination state that represents a local minimum with respect to the figure-of-merit. The ability of the functions to produce a reasonable fit from an initial guess in the iterative curve-fitting process can vary. It is crucial to choose an initial guess that is appropriate based on the physics and chemistry of the instrument and the sample. A poor set of initial guesses can cause the fitting algorithm to direct the fit into a local minimum that is not representative of the sample physics and chemistry. That is, the curve-fitting process can give a mathematically good or even excellent fit even though the component peaks in the final fit are not chemically or physically reasonable.

A figure-of-merit, e.g., χ^2 or the standard deviation of the residuals, is a single number that is often used to guide adjustments to the numerous fitting parameters in the peak fitting process. The fitting process may involve numerous paths though the parameter space with the possibility of hitting and getting stuck in a number of local minima. It is, therefore, possible to obtain a range of outcomes depending on the starting point of the fit. There are a number of additional checks that can be used to ensure that the physicochemical quality of a peak fit is adequate and that the current fit is not just the best mathematical solution. These include the monitoring of the quality of the data reproduction with respect to the noise; the applicability of the curve-fitting model to data of similar origin; the generation of accurate peak areas for spin–orbit components; and the accuracy of peak ratios for peaks from different elements or oxidation states of an element in a known chemical moiety.

Optimization algorithms mathematically fit peaks to data. They lack significant input from physics and chemistry, so optimization based on a single value figure-of-merit may not yield comprehensive, scientifically meaningful results. Physical and chemical information can be added to a peak model through the selection of the lineshapes, the number of component peaks within a peak model, and the parameter constraints, all of which present a means by which known relationships are imposed on otherwise independent

TABLE I. Table of commonly observed errors in XPS peak fitting.

Error	Details	How to avoid	Reference
Labeling noise as chemical components or presenting, fitting, and/or interpreting data that is far too noisy to contain meaningful chemical information	A "sophisticated" analysis does not fix data with a poor signal to noise ratio	Detection limits and signal-to-noise should be sufficient to define component structures within spectra. Estimate the acquisition time per data-bin needed to achieve signal-to-noise required for a scientifically meaningful analysis by peak fitting	Section IV B
Fitting spectral data with a poor energy resolution	A "sophisticated" analysis does not fix data with a poor energy resolution	Data should have sufficient energy resolution to permit meaningful separation of a signal by mathematically fitting of components to data	All examples herein
Truncating the peaks in a narrow scan	Data are taken over a window that is too narrow, which makes it difficult to fit an appropriate *background* and *component peaks*. This includes only utilizing one of the spin–orbit components in a fit	Define energy acquisition regions of sufficient width to include surrounding noise and the leveled-off background. Include all components of spin–orbit splitting and satellite peaks, unless the shift is too large for a reasonable narrow scan, e.g., the Co 2p signals have a shift of 15 eV, which would fit in a typical narrow scan	All examples herein
Neglecting to include a *background* or using an inappropriate *background* for the fit	This can change the area under the curve and, therefore, the ratios of the fit *component peaks*	The inelastic background is an integral part of a peak model. Background selection should be based on the physical properties of the materials analyzed and should be justified	Section IV G and Background correction guide[8]
Failing to make the *background* match the surrounding noise/spectrum	This can change the area under the curve and, therefore, the ratios of the fit *component peaks*	The background needs to connect a spectrum with the noise level surrounding it, using an average to find the middle of the noise. In some cases, the background may fall slightly below the noise on one or both sides of the peak	Section IV G and Background correction guide[8]
Having widely varying peak *widths* in a fit without chemical reason	This mistake often results from neglecting to restrain the FWHM values of the fit components. This error can drastically change component percentages	Understand contributions of experimental and fundamental parameters into the FWHM, refer to the literature to determine appropriate FWHM, determine FWHM values experimentally, and use constraints to keep FWHM values within a small range, two rules of thumb are ±10% of FWHM and ±0.1 eV	Section IV E

TABLE I. (*Continued.*)

Error	Details	How to avoid	Reference
Mistreating spin–orbit splitting or neglecting spin–orbit splitting	This mistake involves disregarding spin–orbit splitting, neglecting to use the proper intensity ratio for a pair of spin–orbit split peaks, and/or only considering spin–orbit splitting for a fraction of the fit components that need it in a peak envelope. In many cases, spin–orbit peaks are incorrectly labeled as separate chemical states	Area and position constraints for doublet peaks are well defined and should be used when constructing peak models that include doublet pairs. Use reference databases for understanding expected spin–orbit properties such as energy splitting, intensity ratios, and FWHM differences. Use constraints to define the properties of the synthetic peaks	Section VI C
Adding too many synthetic *component peaks* to a fit	More peaks will generally "improve" a fit, but they may not have chemical meaning or statistical validity. The lower limit for a plausible FWHM is determined by the energy resolution for an instrument	Only assign core level shifts to possible chemical and physical contributions. Use complementary data from other analytical techniques to understand the different chemistries possible. Determine the energy resolution for the operating mode used to acquire spectra. Use databases for accepted chemically meaningful curve fits of reference materials. The number of components used to model a given data envelope should be consistent with data collected from related photoemission lines from the same sample measured at the same time (i.e., C—O peak should be confirmed by both C 1s and O 1s spectra)	Section VI
Failing to include the original data, only showing smoothed data, or only showing *component peaks* and perhaps their sum as the original spectrum	This mistake makes it impossible to evaluate the quality of the original data or the fit to it	The original, unsmoothed data should be shown. The individual synthetic component peaks, the sum of the synthetic components, and the residuals should also be shown	All examples herein
Using incorrect lineshapes—ignoring asymmetry and variability of Lorentzian/Gaussian character	Choice of lineshapes affects the relationship between components and relative areas of component peaks	The choice of the lineshape depends on the type of material being analyzed. The selection of lineshape is a form of constraint placed on components in a peak model	Section IV D
Not showing the *residuals* to the fit, and/or a figure-of-merit for the goodness of the fit	Excluding this information makes it difficult to determine the quality of the fit	The reported/plotted data should include the residuals to the fit. It is also helpful to provide a figure-of-merit for the goodness of fit, especially	All examples herein

TABLE I. (*Continued.*)

Error	Details	How to avoid	Reference
		when multiple spectra are shown/compared	
Mislabeling or not considering the relevant physics and chemistry of the spectra when identifying peaks	Some examples of mistakes here include (1) shake-up (satellite) peaks identified as chemical states in sp^2 carbon, e.g., in nanotube or graphene-based materials, (2) synthetic peaks corresponding to metals or materials with sp^2 carbon represented as symmetric when asymmetry would be appropriate, and (3) ignoring other information from the XPS analysis, e.g., including peaks for oxidized carbon when no oxygen is present in a material	Use reference databases that describe all spectral features for reference materials. Measure data from standard samples to verify the performance of an instrument and understand the limitations of XPS when analyzing similar materials of known composition. Where appropriate, use the data acquisition parameters in the references/database	Sections VI A and VI B
They are mislabeling higher oxidation states incorrectly as coming from lower oxidation states	This sometimes occurs in C 1s peak labeling, where labels for the C—O and C=O fit components may be reversed, or a carboxyl signal may be mislabeled as a carbonyl	Use reference databases that describe all spectral features for reference materials. Measure data from standard samples to verify the performance of an instrument and understand the limitations of XPS when analyzing similar materials of known composition. Where appropriate, use the data acquisition parameters in the references/database	Sections VI A and VI B

component peaks. That is, the likelihood of achieving a chemically reasonable fit is increased if the initial guesses are based on solid scientific principles.

The art of fitting data with peaks is in selecting the appropriate number of component peaks, making use of appropriate lineshapes, and limiting the set of fitting parameters through parameter relationships to produce peak models capable of measuring physically meaningful quantities from XPS spectral forms. The challenging part arises in selecting the correct physical solution from the set of potential mathematical solutions. In practice, this is best done by obtaining verification of the fitting model by repeating these measurements on equivalent samples to confirm that the observed changes are representative of the samples. Data collected should include measuring data from standard samples to verify the performance of an instrument and understand the limitations of XPS when analyzing similar materials of known composition.

III. COMMON MISTAKES IN XPS PEAK FITTING

Following the principles outlined in this guide should help the analyst avoid many of the errors listed below. Nevertheless, these errors are regularly seen in the scientific literature.[3] Of course, there are many examples in papers of proper XPS analysis and

peak fitting that include appropriate considerations of the physical and chemical nature of the relevant spectra. Some of the errors listed below are superficial and do not impact the conclusions of a paper. However, some fundamentally alter the interpretation of the data and the conclusions drawn from it. Table I lists the errors in XPS peak fitting that we have observed in the scientific literature and suggests ways to avoid them. A more detailed discussion of the errors can be found in a report.[7]

IV. XPS MEASUREMENT

The chemical information that can be determined from curve-fitting XPS spectra can only be physically meaningful if the data are appropriately collected, and proper consideration is made of all the physical and chemical contributions to the photoelectron spectra.

A. Instrument calibration and performance

Energy calibration of the instrument is a prerequisite for accurate peak energy identification. Any instability within an instrument has the potential to alter lineshapes and accurate kinetic energy registration. Regular instrumental calibration and check-up

are critical to ensure that the instrument is performing within the acceptable limits of reproducibility and accuracy[9] needed for physically meaningful interpretation of curve fit results of spectra.

Figure 1 shows two Nb 3d photoemission spectra collected from a sample that was mainly metallic with a small amount of NbO and NbO_2 present on the surface. The bottom spectrum displayed an incorrect (compressed) spin–orbit splitting for the metallic component and a second component that did not correspond to one of the expected oxide components. These problems were identified by comparison with Nb spectra published in the literature (previously collected data and resources described in Sec. VI A) and were due to a malfunctioning pass energy (PE) control board. The correct spectrum in Fig. 1 (top) has all three expected components (Nb, NbO, and NbO_2).

Even though modern XPS instruments are becoming more stable and reliable, it is crucial to perform regular energy scale and linearity calibrations as prescribed by the standards.[11,12] Recently, a procedure that allows the performance and calibration of an XPS instrument to be checked rapidly and frequently was published.[13]

B. Adequate data acquisition

The quality of information extracted from curve-fitting XPS spectra can only be as high as the quality of the experimental data. The spectra acquired are not always of sufficient intensity and resolution to perform useful peak fitting. Instrumental contributions to the spectrally resolvable chemistries are discussed below. The analyst should also consider the signal-to-noise of the spectra produced. For elements with low sensitivities and/or that are present in low concentrations, overinterpretation of noise as chemistry is a

common error.[3] Another possible error is to acquire data that have a poor signal-to-noise (S/N) ratio and to smooth it before curve fitting. (Note that the S/N ratio varies across an XPS survey spectrum.[3]) Smoothing may introduce changes in the spectral shape and width;[14,15] changing the underlying physics, and may lead to erroneous interpretation of curve fitted spectra.

C. Accurate charge correction

Accurate BE identification relies not only on the instrumental energy scale calibration but also on the accuracy of charge correction if charge compensation is employed during data acquisition. Charge compensation is often required when measuring XPS spectra from insulating materials. A charge builds up near the surface of these materials as the photoelectrons are emitted. This usually shifts the photoelectron energy and distorts peak shape. For details on charge compensation, please refer to the XPS Guide: Charge compensation and BE referencing for insulating samples.[16]

D. Lineshape of an XPS peak

One of the most influential aspects of a successful peak model is the lineshapes or the shapes/functions appropriate for modeling the photoemission process after measurement by an XPS instrument. These lineshapes must accurately represent, or at least closely approximate, the signal measured by an instrument. Therefore, it is essential to understand the role of the instrumentation in modifying peaks.

The XPS process is relatively simple.[17] X-ray light in the intrinsic process causes an electron to move from an initial, occupied energy level to a final, virtual energy level that has energy
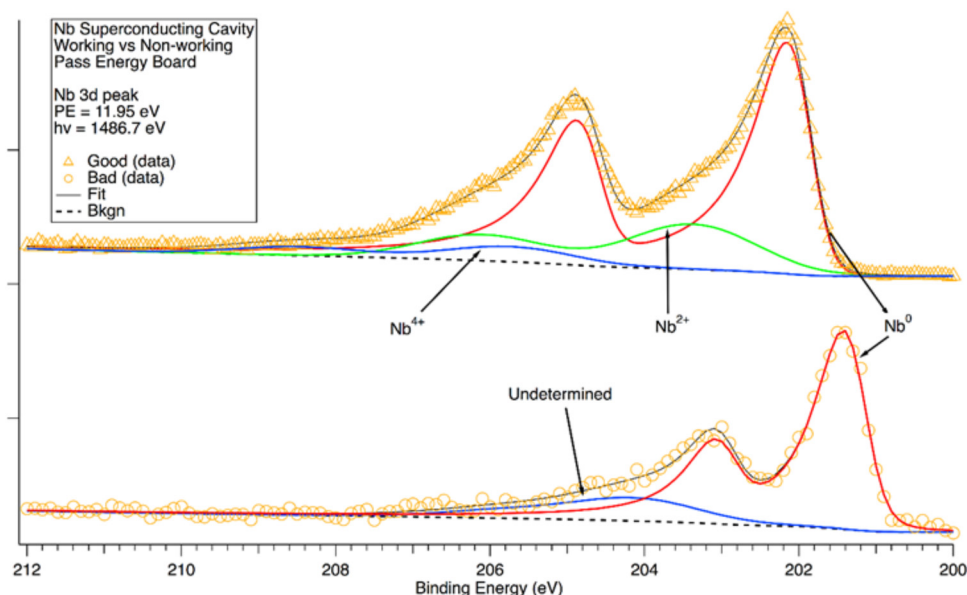
FIG. 1. Nb 3d spectrum collected using a PHI 5600XPS system (Ref. 10). The bottom spectrum was collected with a malfunctioning PE board. The top spectrum was collected after the PE board had been replaced. A Shirley background was used.

greater than the Fermi level of the solid under study. The electron is then lost from the virtual final state energy level and escapes from the solid at a specific energy. This energy is subsequently measured in the spectrometer. The uncertainty principle gives the initial energy level a *Lorentzian* energy distribution (discussed in Sec. IV E). The basic shape of the XPS peak recorded in a spectrometer is modified by instrumental and other factors (such as phonon broadening) to give a *Gaussian* contribution.[18] This leads to a measured lineshape that is a convolution of a Gaussian and a Lorentzian function. This function, known as the *Voigt* function,[19] most accurately reflects the nature of this intrinsic XPS process.

XPS peaks can be expressed by Voigt functions that vary in their amounts of Gaussian and Lorentzian character. This can be done by identifying a Gaussian (*ghm*) and a Lorentzian (*lhm*) FWHM.

A parameter called the "Gaussian/Lorentzian mix," *glmix*, may be defined as

$$glmix = \frac{lhm}{lhm + ghm},$$

which takes the value 0.0 for a pure Gaussian and 1.0 for a pure Lorentzian. Thus, the Voigt function varies the amount of Gaussian and Lorentzian character by using Gaussian and Lorentzian FWHM values that are usually different. Figure 2 shows a plot of the Voigt function with *glmix* = 0–0.9999. It should be noted that Gaussian–Lorentzian sum and product functions, which approximate the Voigt function, called pseudo-Voigt, have also been widely used in XPS peak fitting.[20] In these pseudo-Voigt functions, there is a mixing ratio (M), which controls the amount of Gaussian and Lorentzian character, typically M = 1.0 for a pure Lorentzian and M = 0.0 for a pure Gaussian, but sometimes these M values are reversed. As discussed in Sec. IV F, extrinsic, as well
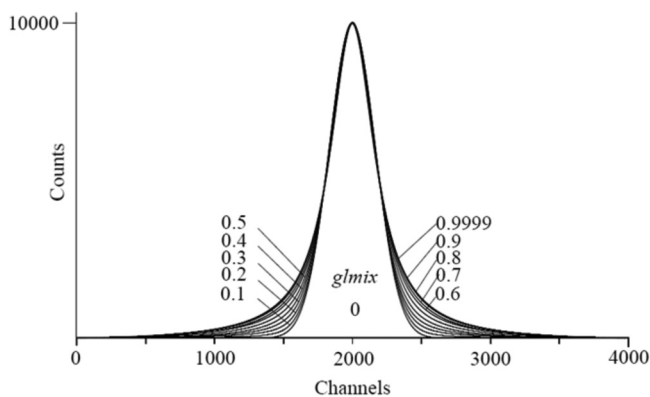
FIG. 2. Plot of Voigt functions that can be used to describe the shape of XPS peaks. The functions are calculated for a single peak with an FWHM of 400 channels and a peak maximum of 10 000 counts over a range of 4001 channels, 2000 channels to the right and left of the peak. When these parameters take a value of 0, the peak is a pure Gaussian. When they take a value of 1, the peak is a pure Lorentzian (Ref. 21).

as additional intrinsic, processes can occur after the intrinsic XPS process that can give additional spectral features.

In choosing a Gaussian–Lorentzian mix, it is important to note the following points:

- Typically, it is found that compounds have a more Gaussian peak shape than metals, which usually have considerable Lorentzian character. One reason for this is the presence of optical phonons in compounds, whereas metal has principally low-energy acoustic phonons leading to an increase in vibrational broadening in compounds and thus more Gaussian character. This topic is discussed in Sec. IV E.
- In the curve-fitting process, the analyst starts the process by suggesting possible values for the various peak parameters such as BE, FWHM, Gaussian/Lorentzian character, and peak heights. It is usually necessary to fix some of these parameters in order for the iterative process to converge. The analyst will determine typical values for Gaussian–Lorentzian mix for their instrument, but typical values for many instruments are given below:
  ○ Compounds: *glmix* below 10% for Voigt functions and M = 0.5 for pseudo-Voigt product functions and M = 0.2 for pseudo-Voigt sum functions.
  ○ Metals and elements: *glmix* above 60% for Voigt functions and M above 0.8 for pseudo-Voigt functions and M above 0.6 for pseudo-Voigt sum functions.

These represent good starting guesses for the Gaussian–Lorentzian mix values.

E. FWHM of the XPS peak

The FWHMs of the Voigt function peaks used in core XPS peak analysis depend on several factors discussed below.

1. Lifetime of the core hole—the natural linewidth

The photoelectron peak is broadened to give a Lorentzian shape that depends on the lifetime of the core hole resulting from the photoelectron process. The core hole corresponds to an excited state, and various processes fill this hole, especially x-ray or Auger emission. There are several tabulations (Refs. 22 and 23 and references therein) of natural linewidths, a number of which are based upon experimental data from x-ray emission spectroscopy and Auger spectroscopy and calculations. Krause and Oliver published[23] a tabulation of core energy levels from atomic number 10 to 110, and many other papers report natural linewidth values, including those using XPS data.[22]

2. Linewidth of the x rays used to eject the photoelectron

The natural linewidth of core energy levels increases as the binding energy, BE, of the core energy level increases. Thus, the linewidth of the Kα$_{1,2}$ x-ray emission lines increases as the atomic number (Z) of the x-ray target increases (by a factor of Z^4) for the K lines.[24] For example, aluminum Kα x rays have a much narrower linewidth than higher energy chromium Kα x rays. Higher energy x-ray sources are used in hard x-ray photoelectron spectroscopy, abbreviated as HX-PES or HAXPES. Photoelectrons from deeper

core levels can be excited by higher energy x rays compared to soft Al Kα x rays. For example, for Al, a soft x ray can excite up to the 2s orbital only, but a hard x ray can excite up to the 1s orbital.

Figure 3 shows the Al 2p and Al 1s core regions obtained using a Cr x-ray source, which has an energy of 5414.7 eV. The kinetic energy of Al 2p photoelectron is ~5336.8 eV, which is much higher than the kinetic energy of Al 1s electron (~3850.3 eV). The spectra in Fig. 3 are overlayed to the same maximum and intensity for comparison. In Fig. 3(a), the Al 2p curve fitted with two asymmetric spin–orbit components separated by 0.44 eV and at 2:1 intensity ratio. The causes and treatment of asymmetry are discussed in Sec. VI F. In Fig. 3(b), Al 1s and Al $2p_{3/2}$ components of Al 2p transition are overlayed to the same maximum and intensity for comparison. The FWHM of Al 1s spectrum is 1.35 eV while that of Al $2p_{3/2}$ component is 1.08 eV, demonstrating the increase of lifetime broadening for the deeper core level.

3. Effect of the spectrometer used to measure the photoelectron energy on the linewidth

The spectrometer that measures the kinetic energy of the photoelectrons adds additional width to the natural linewidth, as well as giving Gaussian character to the peak lineshape. This means that the observed linewidth is generally substantially different from the natural linewidth necessitating the use of the Voigt function described above. Tables of natural linewidth (e.g., Ref. 22) can be helpful in setting the Lorentzian component of the Voigt function in a curve fit of a spectrum but rarely describe the measured peaks themselves. Typically, the analyst should obtain the spectrum with the best resolution available from the specific spectrometer,

consistent with a balance between the appropriate signal to noise ratio and analysis time available, used to get the best data for curve fitting.

4. Resolution of the spectrometer used to measure the photoelectron energy

Most XPS instruments use hemispherical analyzers. Usually, the photoelectrons have their energy adjusted in a lens system so that they enter the hemispherical analyzer with particular kinetic energy called the PE. The analyzer settings, including PE, contribute to the resolution function of the instrument and hence to the energy resolution and photoemission peak shape. Therefore, it is important to determine the energy resolution for the operating mode used to acquire spectra that will be curve fitted.

5. Chemical environment of the atom from which the core photoelectron was ejected

The chemical environment of the atom from which the core photoelectron was ejected has a substantial effect on the FWHM.[4] In particular, the intrinsic photoelectron process couples with phonons in the solid, resulting in broadening of the core peak and giving the peak Gaussian character. Metal phonons are often dominated by acoustic phonons of low energy, whereas metal compounds such as oxides and carbonates have extensive optical phonons of much higher energy resulting from multiple solid-state vibrational modes.[25] Thus, metals normally have substantially narrower FWHM values than metal compounds and more Lorentzian character. Figure 17 in Sec. VI F for the Al 2p region illustrates this
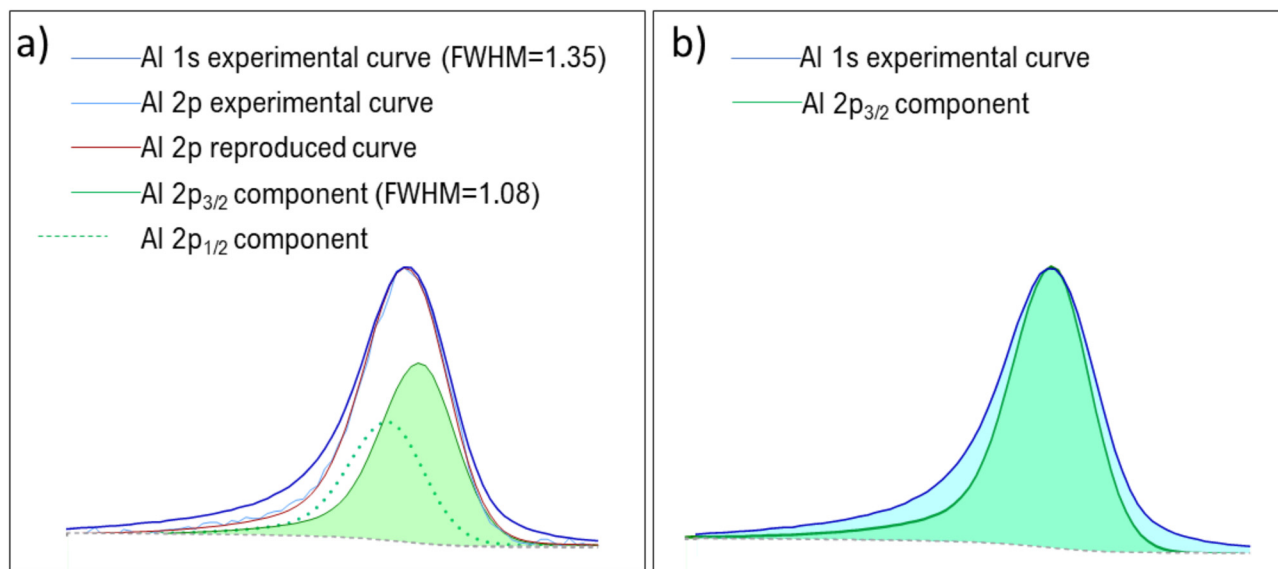
FIG. 3. Core XPS spectra of aluminum metal obtained using Cr Kα photon energy of 5414.7 eV. Spectra obtained using PHI *Quantes* instrument. (a) Al 1s and Al 2p spectra overlayed to the same maximum and intensity for comparison. The Al 2p curve fitted with two spin–orbit components separated by 0.44 eV and at 2:1 ratio; (b) Al 1s and Al 2p3/2 component of Al 2p transitions overlayed to the same maximum and intensity for comparison. A Shirley background was used.

—it can be seen that the oxide peak has a substantially greater FWHM than the metal peak when measured at high resolution.

F. Existence of extrinsic processes as well as additional intrinsic processes

The photoelectron process can be simplified into a three-step model:[26]

- *Step 1*: The excitation of the electron from the initial energy level to the final virtual orbital state. Processes associated with this step are called intrinsic processes.
- *Step 2*: The transfer of the photoelectron to the surface. Processes that occur after the first step are called extrinsic processes.
- *Step 3*: The escape of the photoelectron from the surface into the vacuum.

The first two steps are sometimes called the two-step model.

In addition to the key intrinsic process, there are intrinsic processes that involve the ejection of a photoelectron, as follows.

- *Plasmons*[25] can give rise to additional peaks in a spectrum. Both bulk and surface plasmons are possible. For example, aluminum metal has a rich plasmon structure.[27] Plasmons can also be extrinsic.
- *Shake-up*[5] processes in which a valence electron and a core electron are excited. If the valence electron is promoted to another valence energy level in the sample, this is called a shake-up process. If the valence electron is ejected as an additional photoelectron, the process is called a shake-off process.
- *Multiplet splitting*[5] arises from samples that have unpaired electrons because there is more than one final state depending upon the number of spin up and spin down electrons in these final states. Transition metal compounds are often paramagnetic and, in this case, display multiplet splitting in their core XPS data (discussed in Sec. VI C).
- *High Binding Energy Assymetry*[28] Conduction Band interactions give a tail of approximately exponential shape to the core XPS of conducting materials (Sec. VI F).

Extrinsic processes include

- *Plasmons*, which can also be intrinsic.
- *Inelastic processes* often occur between ejected photoelectrons and other atoms and molecules. These processes cause loss of energy of the photoelectron and represent the principal contribution to the background in XPS.[29] There are effective software models for the study of this loss structure, and these studies can provide valuable information. These processes can have a large effect on peak ratios as a function of emission angle.

G. Background subtraction

Most XPS spectra have a significant background, and accounting for the background contribution is an important aspect of the curve-fitting process. The choice of the type of background and selection of end points has the most significant impact on the area under the curve, and hence the ratios of the individual peaks used to curve fit the spectrum. There have been numerous studies devoted to approaches for background inclusion, and a forthcoming paper[8] is devoted to this topic. There are three major approaches:

- The removal of the background to yield a spectrum with an approximately horizontal background. This approach alters the experimental data with the subsequent curve fitting being made on the altered data. This can lead to errors depending upon the chosen background model. It also deprives the viewer of the ability to compare the original experimental data with the curve fit. This approach is not recommended.
- The addition of a fixed background to background subtracted spectrum before peak fitting, where this background is not subtracted from the spectrum, and it is shown in the final fit. This approach is mathematically identical to the previous one, but it allows the viewer to see the original data, the background, and the fit together.
- In the *active approach*, the background contains parameters that are included as potentially variable factors in the fit. This method also preserves the data in its original form but allows for different backgrounds in different regions of the spectrum. In some insulators and gases,[30] e.g., in near ambient pressure XPS,[31–34] the XPS background can be linear, but most XPS backgrounds in metals and semiconductors are nonlinear. The active approach allows for addressing these differences in complex materials.

We do caution the reader that a simple linear background between the starting and ending points in a spectrum is incorrect and will cause substantial errors in the peak fitting of spectra where the measured background is not flat. As discussed in the Practical Guides for X-ray Photoelectron Spectroscopy: Quantitative XPS,[35] the line describing the background should, ideally, go through the middle of the noise in the data before and after the peak.

V. EXAMPLE CURVE FIT OF REFERENCE SPECTRA FROM PURE MATERIALS–PET

We fit here a reference spectrum taken at high resolution from an XPS database of organic polymers—PET.[36] PET is an important reference polymer that is used for verifying instrument performance, including charge neutralization validation.[4,13,37,38] Monochromated Al K_α x rays (1486.3 eV) were used to collect these data on a Scienta ESCA300 spectrometer. The energy spread of the monochromator is predicted to be 0.26 eV. A PE of 150 eV was used, and high energy resolution was achieved by using an appropriate analyzer entrance aperture width. The FWHM of the C 1s envelope was determined to be 0.67 eV. Low-energy electrons were used for charge compensation.

The PET structure is shown in Fig. 4. Based on its chemical formula $(C_{10}H_8O_4)_n$, there is 71 at. % of C and 29 at. % of O in PET. There are 10 carbons in the repeating unit of the polymer, 4 of which are present in the aromatic ring (labeled 1) with a BE of 284.7 eV. Two other carbons (labeled 2) in the aromatic ring are secondary shifted carbons such as C*—C(=O)O, which will contribute to the BE of ~285.3 eV. Two carbons that are singly bonded to oxygen (labeled 3) have BE of 286.2 eV. The other two carbons are in carboxyl (ester) groups (labeled 4), and their BE is 288.7 eV. Out of the four total oxygens, half are present in the O=C part of the carboxyl/ester group (labeled 1) at 531.6 eV, and the other half are in the O—C part of the carboxyl/ester group (labeled 2) at 533.2 eV.
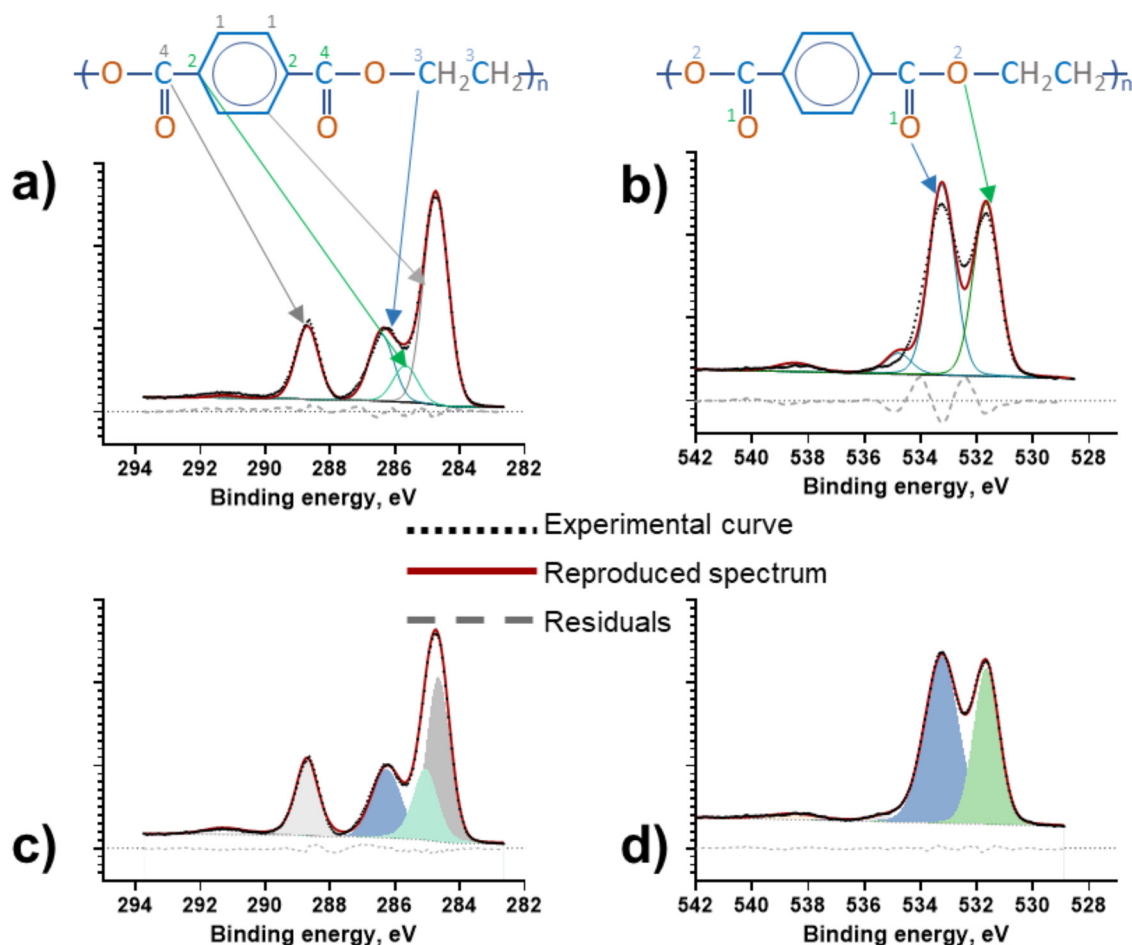
.... Experimental curve
—— Reproduced spectrum
— — Residuals

FIG. 4. High-resolution C 1s and O 1s spectra of PET fitted using symmetrical GLS (fixed M = 0.1) peaks. (a) and (b) Initial set of peaks added to initiate the curve fit. (c) and (d) Final curve fitted spectra. Residuals are displayed below the spectra. A Shirley background was used.

The C 1s and O 1s spectra are accompanied by a survey scan confirming that no other elements are present at the PET surface. When a Shirley background is used for quantification of the high-resolution C 1s and O 1s spectra, 69 at. % C and 31 at. % O are detected. Slightly different concentrations due to the possible presence of adventitious carbon[38] are observed.

Figure 4 shows C 1s and O 1s high-resolution spectra (narrow scans) with component peaks added to initiate a curve fit. The original data from the "High Resolution XPS of Organic Polymers: The Scienta ESCA300 Database"[36] have been fit using the commercial software MultiPak 9.9.[39] Four component peaks are added to the carbon spectrum, reflecting the number of different chemical environments that contribute to the resolvable BE shifts discussed above. Due to the aromatic structure of the benzene ring, a shake-up signal is observed above 290 eV, which should represent ca. 7% of the total carbon signal based on the reference data.[36] This shake-up contribution is fit with one or more peaks.

Once the necessary component peaks have been added into the envelope, constraints on the adjustable parameters need to be established. If the goal is to understand the chemical state information in the spectra, adding parameter constraints will improve the stability of the peak model with respect to the noise. However, with each new constraint, the output from the optimization converges ever more closely to the solution defined by these constraints until the usefulness of fitting peaks to the data is lost. If the goal is to measure the intensity changes for a series of samples from the same study and a peak model is well formed, then a rigid peak model that is heavily constrained will tend to return more consistent intensities for data with similar chemistry and experimental conditions. Somewhere near the middle of these two extremes is the domain for most photoemission peak fitting.

FWHM constraints and the indirect constraints imposed by lineshape selection are the two main parameters used in peak fitting. Other types of constraints, such as spin–orbit intensity ratio

for spin–orbit splitting, are discussed in Sec. VI C. For spectra with well-defined peak resolution, e.g., the C 1s narrow scan of PET, the FWHM can be chosen based on the widths of the individual peaks to reproduce the experimental curve as best as possible. Some variation (ca. 10% of the FWHM or ±0.1 eV) might be justified among different peaks due to small secondary effects. As described above, a function having both Gaussian and Lorentzian character often best describes the experimentally derived spectra. The pseudo-Voigt function that is used to approximate the Voigt function is typically either a product function or a sum function. Both functions involve the mixing of equal width Gaussian and Lorentzian functions with a mixing ratio (M) defined in the analytical function. The mixing ratio, M, takes the value 0.0 for a pure Gaussian and 1.0 for a pure Lorentzian, though some authors have the reverse definition. During the iterative fit, a fixed GL mixing ratio can be chosen, or a range of GL mixing ratios can be used during optimization to find the best fit. In this example, a sum function of Gaussian and Lorentzian (GLS) with M = 0.1 (where M = 0.0 is for 100% Gaussian) was used.

Similarly, based on the sample chemistry, two peaks to be fit are added to the O 1s spectrum to best approximate the number and type of chemical moieties present. That is, as predicted by the chemistry of PET, the O 1s spectrum is fit with two distinct peaks of approximately equal height and similar FWHM. Due to the aromatic structure of the benzene ring, some shake-up signature is observed above 539 eV. One more peak is added at ca. 535 eV to account for surface contamination.

During an iterative fit, constraints of FWHM and lineshapes are used to minimize the residuals—the difference between experimental and fitted curves. It is good practice to show the residuals of a fit. Figure 4 and Table II show the final parameters used to fit the spectra. The percent area obtained is slightly different from the data published in the Handbook due to the different lineshapes used in the original Handbook.[36] The resulting peak model consists of the peak position and percent area that each component peak occupies out of the total carbon signal. The component peak position information is then translated into the chemical state of the sample. Curve fitting of the C 1s spectra results in 40.3% of the area coming from C^1 (284.8 eV), 20.2% from C^2 (285.3 eV), 20.2% from C^3 (286.3 eV), and 19.3% from C^4 (288.7 eV) (with shake-up peak at 291.3 eV excluded from the total area). Curve fitting of the O 1s spectra results in 42% of the area coming from O^1 (531.7 eV)

and 58% from O^2 (533.2 eV) (with shake-up peak at 538.5 eV and contamination peak at 535.0 eV excluded from the total area).

Based on the area under each component peak, the quantification of PET can be derived, as shown in Table II. This direct, quantifiable comparison of the carbon and oxygen in the polymer can be used to confirm both the structure of the polymer and that the curve fit adequately reflects the chemical structure.

VI. AVOIDING MISTAKES DURING PEAK FITTING

A. General information and databases of reference spectra with information on peak widths, separations, and satellite positions

There are several resources available to assist in curve fitting, including complex spectra that contain several chemical components. The NIST XPS database[40] and XPS Spectra (Chemical Shift/Binding Energy)[41] are searchable databases containing line positions, chemical shifts, values for doublet splitting, and energy separations of photoelectron and Auger-electron lines. X-ray Photoelectron Spectroscopy (XPS) Reference Pages[42] and the XPS Reference Table of Elements[43] contain curve-fitting details, BEs, FWHMs, spin–orbit splitting values, references, and other practical notes for most of the elements in the periodic table. The XPS simplified website also contains useful information for narrow scan analysis.[44]

There are various valuable databases that contain high-quality spectra of known materials that can be downloaded. These include:

- Representative spectra for each element in a book published by Physical Electronics and used by analysts for many years.[10]
- The journal *Surface Science Spectra* (*SSS*). This journal has an invaluable collection of spectral data with full experimental details. From volume 15 onwards, data can be downloaded as a text file. SSS contains many examples of peak fitting.
- *eSpectra*[45] is a database and comparative tool that contains the complete collection of the spectra published in *Surface Science Spectra* as well as from other sources.
- The XPSSurfA database hosted by La Trobe University in Australia contains spectra from high-quality samples that were collected under precise conditions.[46]

TABLE II. Parameters used to curve fit C 1s and O 1s from PET in Fig. 4.

	C 1s				
BE, eV	284.8	285.3	286.3	288.7	291.3
FWHM, eV	0.9	1.0	1.2	0.9	2.5
% Area	39.4	19.7	19.7	18.9	2.3
% Area without a shake-up	40.3	20.2	20.2	19.3	0.0
	O 1s				
BE, eV	531.7	533.2	535.0	538.5	
FWHM, eV	1.1	1.4	1.4	2.0	
% Area	39.6	55.9	2.0	2.8	

B. Use of reference spectra

1. Resolving overlapping peaks

In this example, the N 1s spectrum of N-doped HfO_2 overlaps with the Hf $4p_{3/2}$ region. The Hf $4p_{3/2}$ peaks appear between 375 and 390 eV, while some higher BE components contribute to the energy range where a signal from N 1s is expected. To solve this problem of overlapping spectra, it is important to acquire the spectra from the reference material, a thick Hf oxide film without nitrogen doping in this case. Figure 5 shows a high-resolution Hf $4p_{3/2}$ region in which several peaks are included to fit the experimental data.

The Hf $4p_{3/2}$ region [Fig. 5(a)] has features that occur in the same region where N 1s signal is present. In this example, the purpose of curve-fitting Hf $4p_{3/2}$ spectrum is not to extract the chemistry of Hf but rather to create a mathematically rigid model in which peaks overlapping with the N 1s region are constrained in position, width, and area to the higher intensity peak in the lower BE region which is free of overlap with the N 1s region. Two peaks due to Hf $4p_{3/2}$ in the region where N 1s is located, i.e., between 390 and 405 eV, are constrained in intensity, position, and width with respect to the most intense peak at 383 eV. For an N-doped material with two different loadings, the rigid set of peaks is introduced into the high-resolution N 1s/Hf $4p_{3/2}$ region [Figs. 5(b) and 5(c)]. The intensity of peaks overlapping with N is controlled by the height of the most intense peak, and this leads to a poor fit. This fit, though, is consistent with the Hf, so additional peaks must be added to complete a curve fit. These peaks are the contribution from N 1s photoelectrons. This approach is successful even in situations when N loading into the sample is very low, assuming that the data have been acquired with an appropriate signal to noise.

2. Fitting transition metal spectra based on reference spectral envelopes

High-resolution spectra of transition metals are among the most challenging spectra to peak fit.[47–49] Indeed, it is common to see peak fitting of transition metals that oversimplify assignments of peaks to individual chemistries and subsequently have erroneous interpretations of the results. There are several contributing factors

as to why peak assignments are difficult with transition metals. The first is the combinations of intrinsic and extrinsic processes, such as multiplet, shake-up, and plasmon loss structures, contributing to the overall photoelectron shape of the pure metals and their different coordination states. The second is the overlap of the various chemical states usually present in transition metal-based systems. The third is that exposing transient metal compounds to air always results in oxidation and formation of both stochiometric and substochiometric oxidation states. Another complication is that these oxides can have varying degrees of conductivity, which may affect the position and shape of photoelectron peaks due to charging. Early and even current databases, such as NIST and Handbook of X-ray Photoelectron Spectroscopy,[10] usually indicate that there are multiple chemical states that can correspond to the same BE and, at the same time, they provide single BE for a unique chemical environment of the transition metal. However, as multiple reports of reference compounds have shown,[47–49] complex spectral structure, which is the result of an envelope of multiplet peaks and/or other intrinsic and extrinsic effects, is often present with the different chemical states of the element. Simply put, the multiple chemical states of a single transition element often give radically different spectra.

Figures 6(a)–6(c) show spectral signatures for pure metallic Ni, NiO, and $Ni(OH)_2$, as reported by Biesinger et al.[47] The complexity of the spectral signatures due to contributions of the multiple processes that can occur when the photoelectron escapes the 2p orbital is obvious. Therefore, the most accurate approach to solve this problem is to use a curve-fitting parameter either developed by the analysis from pure reference spectra, if they are available, or, to use curve-fitting parameters from reference compounds published in the literature. The first approach is preferred as it ensures that the same spectral and analyzer conditions are used to collect the data from the samples and reference materials. We emphasize that the series of peaks used to fit the narrow scans in Figs. 6(a)–6(c) are simply employed to fit the peak envelope to create an overall shape that will be used in subsequent peak fitting, more than they are intended to have specific chemical meaning.

Figure 6(d) overlays the photopeak shapes (or envelopes) that were created by Biesinger et al. based on fitting the narrow scans in Figs. 6(a)–6(c) for Ni, NiO, and $Ni(OH)_2$.[47] The ambiguity of finding a unique spectral signature for pure reference material is
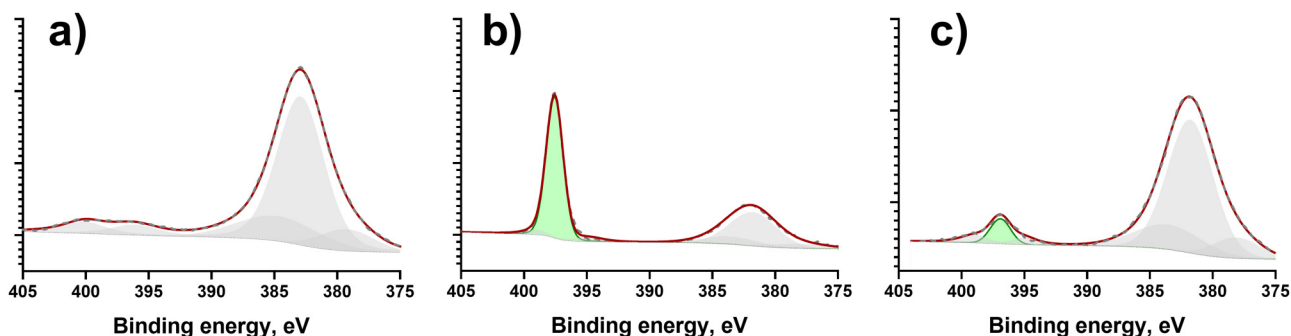

FIG. 5. High-resolution region of Hf $4p_{3/2}$-N 1s electrons for (a) pure HfO_2, (b) highly doped N-HfO_2, and (c) low-doped N-HfO_2. The peak model in (a) is a mathematically rigid constrained model used in separating contribution from the Hf $4p_{3/2}$ region and N 1s electrons in (b) and (c). A Shirley background was used.

obvious. However, through a linear combination of the photoelectron signatures representing the pure chemical states, curve fitting of the mixed chemical states of the transition metals is possible. This is essentially a classical least squares (matrix algebra) problem in which one has the spectrum of the mixture of compounds as well as those of the pure components.[50] Figure 6(e) shows a curve fit of the spectrum from a mixed Ni-Mo oxide, which has had the background removed, using this type of complex photopeak model. The relative ratio of the various chemical states of Ni can be extracted from this information, assuming that one knows information on the physical form of the material (powder, spheres, layered surface structure, etc.) supporting the chemical composition derived by XPS fitting.

3. Finding appropriate FWHM values for unknown samples when no references are available

In certain situations, an analyst is confronted with the need to curve fit spectra from complex multicomponent materials where finding appropriate references may not be possible and limited input from other spectral features exists. In this case, care should be taken in deciding physical constraints to be used during the optimization of curve fit parameters.

For most elements, participation in chemical bonding with other elements causes an increase in BE, especially when the elements to which they are bonded are more electronegative. That is, for elements having multiple possible oxidation states, more oxidized chemistries will usually show higher BEs. This pattern is well established for carbon, where an increased number of oxygen atoms bonded to a carbon atom leads to a steady increase in its BE.[6] Here, the presence of more electronegative oxygen atoms deshields the carbon atom, effectively increasing the nuclear charge felt by its electrons, which raises their BEs (and lowers their kinetic energies in XPS). In many cases, the least oxidized (lowest BE) form of an element will produce the "cleanest" peaks in an XPS spectrum that can then be used to select the best FWHM value for the fit. However, this will not always be so—it will depend on the sample chemistry.

Figure 7 shows a high-resolution C 1s spectrum in which the highest intensity component results from the contribution of
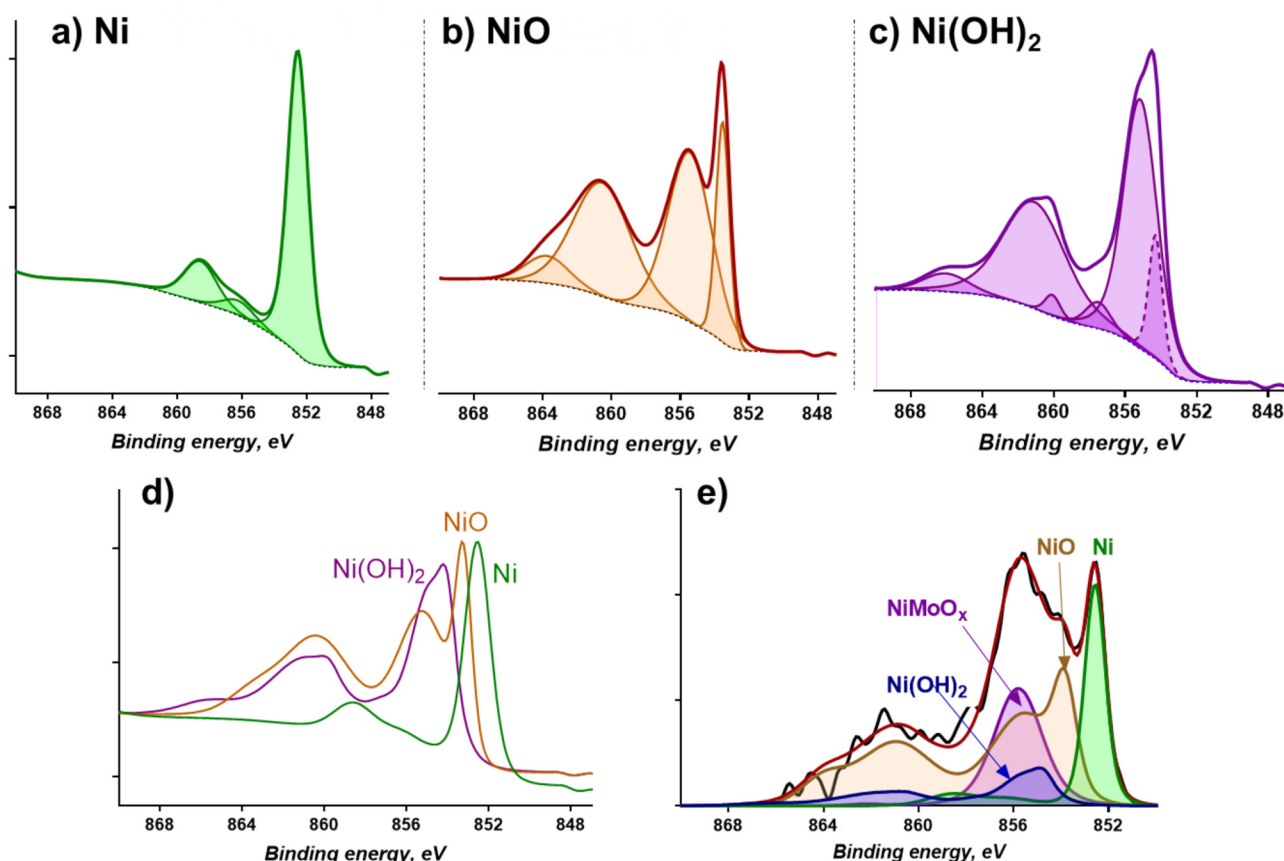
FIG. 6. (a)–(c) High-resolution Ni 2p region for pure reference compounds curve fitted based on Biesinger *et al.* (Ref. 45) peak models; (d) pure reference spectra overlayed; (e) Ni 2p for Ni-Mo oxides fitted using developed peak models. A Shirley background was used.
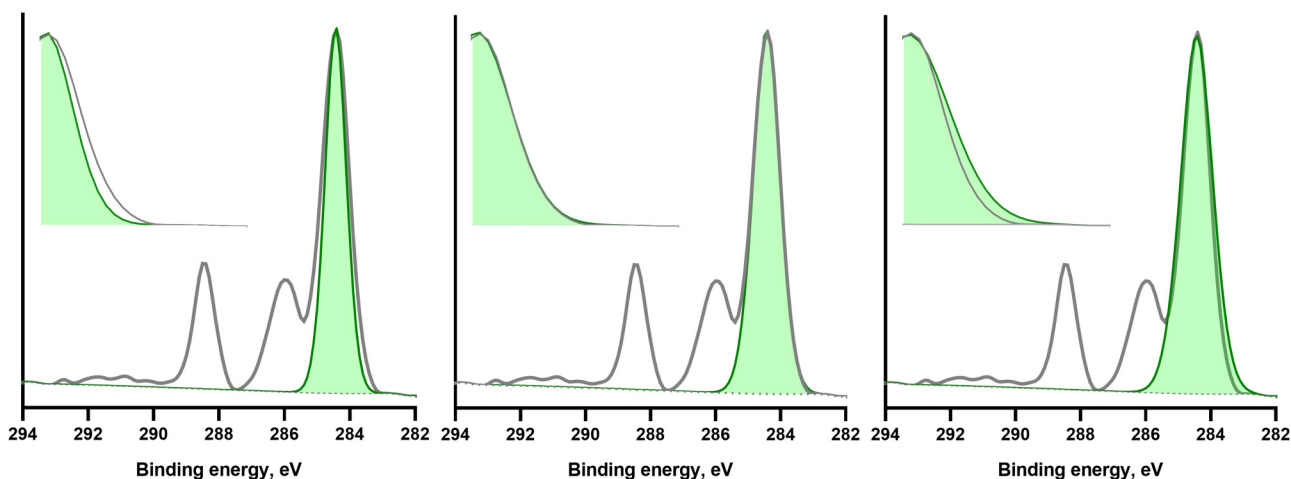
FIG. 7. High-resolution C 1s spectrum of PET fitted using peaks with three different widths to match the right-most slope of the spectrum. Grey—experimental line, green (dark gray)—peak. The upper insets show zoomed-in areas between 282 and 284.5 eV. The linear background was used.

carbon in the lowest oxidation state in the material, which is also the most abundant. In Fig. 7(a), the FWHM of the component peak is too narrow, which results in part of the spectral area being under fitted. In Fig. 7(c), the FWHM value is too broad, which results in overfitting the right shoulder of the spectrum. The best match between the component peak and the experimental data is shown in Fig. 7(b). The FWHM value obtained from this match is probably an adequate representation of the physical, chemical, and instrumental contributions to the data. To a good first approximation, this FWHM could be used for other component peaks that might be considered in the fit. Nevertheless, the lone peak at ca. 289 eV in this spectrum is another reasonable choice for determining the FWHM values of the fit components—it seems to have far less overlap with other signals than the larger peak around 284.5 eV. It would be advisable to consider both FWHM values in this curve fitting (they should be quite similar). Further analysis would be needed to determine which would be most appropriate, or their average, range of values near the average, etc.

C. Spin–orbit splitting ratio and energy separation

Area parameter constraints are particularly useful for spin–orbit peaks, which are doublet peaks originating from the same electron configuration initial state where the final state electronic configuration is split between two possible outcomes. Physics for the photoionization of electrons dictates these double peaks appear offset in energy, representing the difference in energy between the final states and at a defined ratio in terms of peak area (inset, Fig. 8). Scofield cross sections[51] were calculated for photons with energies corresponding to Al and Mg x-ray gun anodes, and these cross sections include relative intensity values for both peaks in a doublet pair. Thus, the ratio for these peaks can be readily fixed by making use of Scofield cross sections to estimate the relative area imposed by area constraints within a peak model. Figure 8 shows the S 2p spectrum that was fitted with two sets of doublet peaks.

The separation between the 3/2 and 1/2 components of the S 2p orbitals is fixed to 1.16 eV, and so is the area ratio to 1:2.

It is worth noting that in the case of p, d, and f levels, spin–orbit splitting occurs, and in a number of cases, the FWHM value of the higher BE component is greater than the lower BE component, an effect which has been described as a Super Coster–Kronig effect.[52] When the FWHM of spin–orbit split components differs, it is essential that the curve-fitting program has the capability of

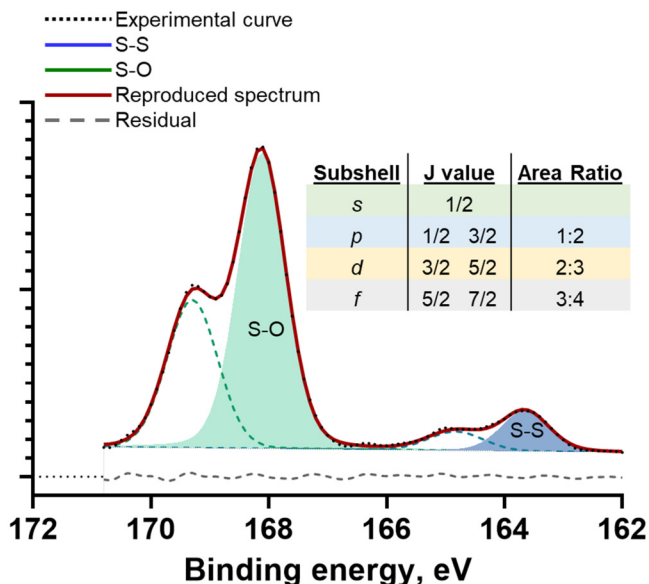| Subshell	J value		Area Ratio
s	1/2		
p	1/2	3/2	1:2
d	3/2	5/2	2:3
f	5/2	7/2	3:4

FIG. 8. High-resolution S 2p spectrum fitted with two doublets separated by 1.16 eV and area ratioed to 1:2 to each other. A Shirley background was used.

TABLE III. Spin–orbit splitting for common transitions.

	Metal	Oxide
Ti 2p	6.1	5.7
Si 2p	0.63	N/A
Fe 2p	13.1	
In 3d	7.6	
Mo 3d	3.15	
Ag 3d	6.0	
Au 4f	3.7	
Hf 4f	1.68–1.71	
Pt 4f	3.35	

FIG. 9. Crystalline molybdenum dioxide (Mo^{4+}) with contamination from Mo^{6+}. The peak model involving these three sets of doublet components includes an example of an active approach to modeling background signal. The component shapes used to the model background are exponential decay curves convoluted with a Lorentzian.

setting the FWHM of the spin–orbit components to an adjustable ratio while keeping the peak areas in the expected area ratio.

Table III shows energy separation for a few common transitions. For some transitions, such as Ti 2p and Si 2p, there may be a difference in separation for different chemical states. For example, spin–orbit energy separation is smaller for Ti oxide than for metal, while spin–orbit splitting is only used in fitting metallic Si and not higher oxidation states. The separation may be smaller than energy resolution or as large as 20 eV.

For elements like the transition metals with a rich range of oxidation states, e.g., Mo, there may be challenges using a single doublet for each chemical state. Photoemission from Mo^{4+} is an example of where the relationship between the chemical state and a pair of synthetic components representing a doublet is not appropriate. Following Scanlon et al.,[53] Mo^{4+} is represented by two doublets, while Mo^{6+} is modeled using a single doublet (Fig. 9). It is also an example of where complex data envelopes for a specific oxidation state are essential for correlating the amount of substance with intensity derived from synthetic components. That is, the amount of material calculated for Mo^{4+} requires the summation of the signal corresponding to four synthetic components labeled [1] Mo $3d^{4+}$ and [2] Mo $3d^{4+}$.

In some cases of spectral overlap between two different transitions, the spin–orbit splitting ratio and separation constraints can help resolve overlapping peaks. Figure 10 shows a region in which both Sb 3d and O 1s contribute. That is, the signal from the oxygen photoelectrons overlaps with a larger Sb$3d_{5/2}$ component, while the smaller Sb $3d_{3/2}$ component is free of overlap. In this case, peaks included in the $3d_{3/2}$ region can be a constraint in position and intensity to the peaks contributing to the $3d_{5/2}$ region. Figure 10(a) shows two doublets from the metallic and oxide forms of Sb constrained rigidly between each other. The intensity of the two peaks in the 5/2 part of the spectrum is limited by the intensity of the two peaks in the 3/2 part. A large deviation in the residuals points to where a peak corresponding to O 1s photoelectrons should be included. When the peak due to O 1s photoemission is included [Fig. 10(b)], the contributions of overlapping transitions can be determined quantitatively.

D. Choosing a correct lineshape and background

When selecting lineshapes for use in modeling spectra, one should be aware that the choice of lineshapes has an influence on
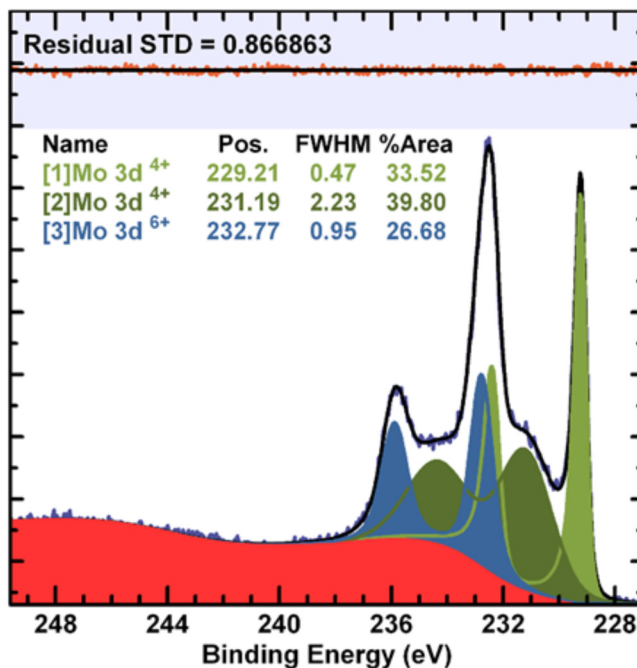
the measured relative area for components in a peak model, and therefore how the signal is allocated to a chemical state. The choice of background also influences the computed areas of the components. A regularly encountered example that illustrates these factors is that of a silicon oxide film on elemental silicon. The Si 2s and Si 2p signals are a useful example because both photoemission lines exhibit features that can be identified as silicon oxide and elemental silicon. They are relatively close in BE and therefore show similar instrumental responses, but they are different in terms of component FWHM and lineshapes. Notably, the Si 2s signal measured on modern instruments with monochromatic x-ray sources shows characteristic lineshapes with wings typically associated with a Lorentzian shape. One way to allow for extended wings in spectral features is to fit basic background curves as part of the optimization step. The Si 2s data in Fig. 11 are fitted using Voigt lineshapes representing elemental and oxide signal plus two lineshapes with background characteristics. A component in the peak model is used to emulate a Shirley response to model inelastic scattering due to elemental silicon. At the same time, an offset summed with the Shirley background is defined by making use of a top-hat lineshape of width greater than the energy interval shown in Fig. 11 that is adjusted to allow the use of Voigt lineshapes when the fitting is performed.

In the case of the silicon dioxide overlayer on silicon, the Si 2p and Si 2s core level measurements should return equivalent corrected areas for component peaks. An equivalent model for Si 2p
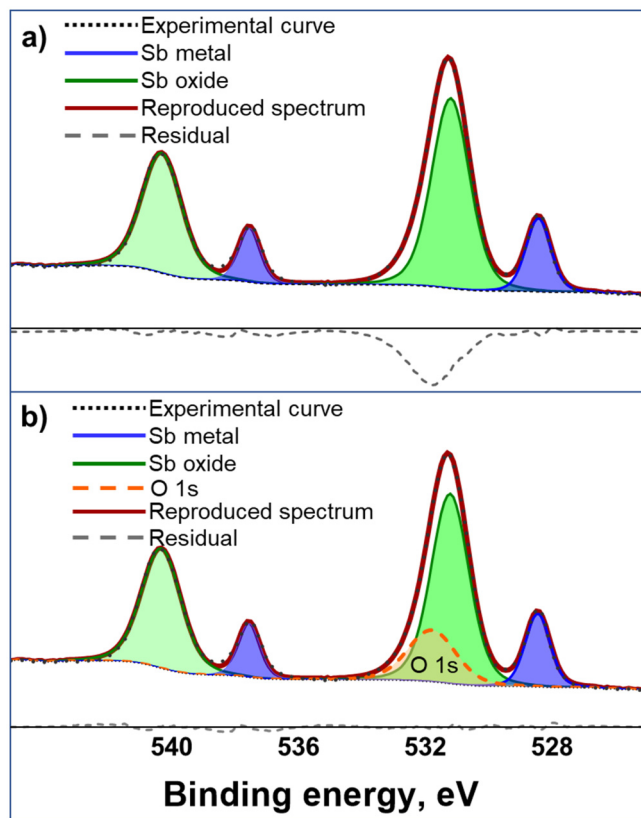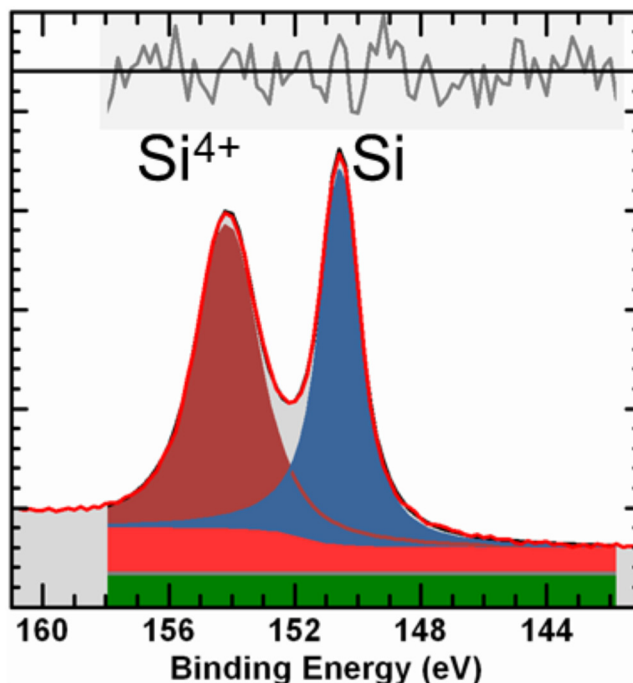
FIG. 10. O 1s/Sb 3d region. (a) Two doublets used to fit Sb 3d contributions by constraining the intensity, position, and width of the peaks in the 5/2 region with respect to those in the 3/2 part. A high negative residual in the range of 530 eV is seen; (b) a peak due to O 1s electrons (dashed) must be included to accurately complete the curve fit. A Shirley background was used.
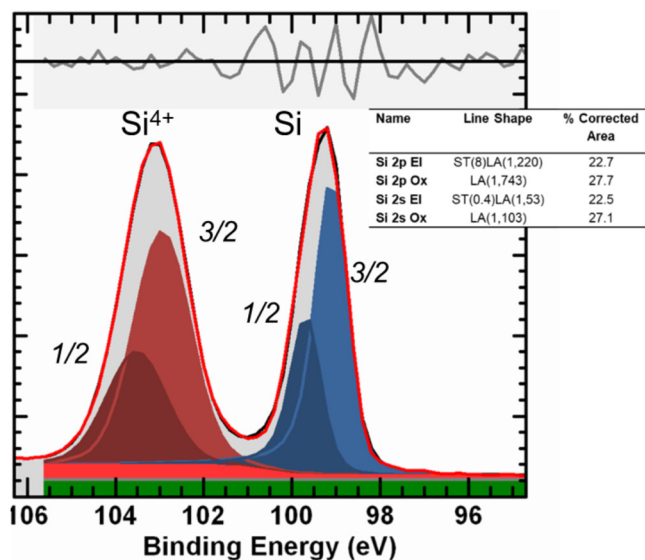

FIG. 11. Si 2s measured using a PHI Quantum 2000 monochromatic Al x-ray source with pass energy 46.95 eV from a sample consisting of a 4 nm thick silicon oxide layer over a substrate of elemental silicon. A horizontal background is offset from the data (green zone, lowest intensity section). Two curves (bright red) fitted during optimization representing background signal in addition to the green zone are defined as a Shirley background generated by the elemental silicon component (blue, lowest BE peak) and a top-hat lineshape, the height of which allows lineshapes of significant Lorentzian character to be used to model both elemental Si 2s and oxide Si 2s intensity.

to that of Si 2s is used for curve fitting. The principal difference between Si 2p and Si 2s is that Si 2p involves doublet peaks with significantly less Lorentzian character. Nevertheless, both peak models in Figs. 11 and 12 provide excellent data reproduction, and the use of these lineshapes is supported by observing the consistency achieved for chemical state component areas calculated from these peak models (inset table in Fig. 12). The asymmetric Lorentzian (LA) lineshape used in this example is described in detail in recent reports.[54,55]

E. Including shake-up

For unsaturated carbon, which is often in aromatic rings, a shake-up feature due to π–π^* (HOMO–LUMO) transitions coming from the ring excited by the exiting photoelectrons must be considered.

A peak model for PEEK (Fig. 13) includes features assigned as shake-up signals typical of ring polymer spectra. The use of shake-up components in a peak model for PEEK is particularly important for modeling the O 1s signal since a shake-up feature is potentially beneath signal attributed to O—C O 1s. PEEK spectra are

comprised of core photoelectron peak, shake-up, and inelastically scattered background signal. Accounting for these three sources of the signal is fundamental to accurate quantification by XPS.

F. Asymmetry parameters for metals and aromatic structures

Asymmetry is observed in photoemission data for a number of reasons. The origin of this asymmetry is multifaceted, including instrumental influences, sample/measurement artifacts, the band structure of the sample, and other physical reasons associated with photoemission itself. Modeling asymmetric components is arguably one of the more difficult problems related to peak fitting.[54,57,58]

Historically, asymmetry has been included in lineshapes via a so-called exponential tail. The necessary form for including an exponential tail is produced by blending the influence of an exponential function with a lineshape with characteristics of a Lorentzian and/or a Gaussian resulting in a well-defined component area. Figure 14 illustrates one possible form for exponential tail modification to a Lorentzian lineshape, which was extensively used when fitting polymer spectra within the Beamson and Briggs

Name	Line Shape	% Corrected Area
Si 2p El	ST(8)LA(1,220)	22.7
Si 2p Ox	LA(1,743)	27.7
Si 2s El	ST(0.4)LA(1,53)	22.5
Si 2s Ox	LA(1,103)	27.1

FIG. 12. Si 2p data measured consecutively with the Si 2s data in Fig. 11 modeled using lineshapes shown in the inset table that differ significantly from those used for Si 2s. The background is approximated using a flat pedestal background upon which a component formed by computing a Shirley background making use of elemental silicon components to compute the shape for the Shirley response. The definition of lineshapes is described in Casa Software manual (Ref. 56). Quantification is performed with Scofield cross sections. The Effective Attenuation Length (EAL) Universal formula and the transmission function are defined by PHI.

XPS of Polymers Database.[33] Figure 15 is an example of a peak model consisting of a single component making use of an exponential tail lineshape to fit an O 1s peak measured from Nylon 6 prepared by cleaning with an argon cluster source ion gun.

There are two aspects to fitting data using asymmetric lineshapes, namely, data reproduction and quantification via a comparison of component area. The example shown in Fig. 16 illustrates one of these aspects.

The problematic lineshape used in Fig. 16 is a Doniach–Sunjic profile convoluted with a Gaussian, which certainly allows good data reproduction, but fails to permit accurate quantification as a consequence of an extended asymmetric tail. Care should be taken when using the Doniach–Sunjic lineshape, as component area changes as a function of the asymmetry parameter, and contributions from higher BE components may overlap with an extended tail.

An example of where both data reproduction and quantification are important is measuring intensities for an oxide film over an elemental substrate, such as aluminum oxide on aluminum or silicon oxide on silicon. Separation of oxide signal from an elemental signal is best performed using lineshapes for which adjustments to component parameters do not have significant consequences for the component area, which is not the case for Doniach–Sunjic profiles. For this reason, asymmetry in photoemission peaks is typically modeled using lineshapes other than the Doniach–Sunjic profile.[59]

The case of aluminum oxide on aluminum metal (Fig. 17) is offered as an example of where relating metal and oxide intensities measured by fitting components to data is the basis for estimating a thickness for an oxide film on a metal substrate. In this example, a lineshape is modified to simulate geometric aberration induced asymmetry within measured photoemission lines. Figure 17 demonstrates the use of a subtle but important asymmetry within narrow metallic components. The peak model also includes a background generated by these metallic components, which is modeled with the Shirley algorithm applied to the metallic components only. The oxide background is modeled as linear. The model in Fig. 17 represents a systematic tool for comparing intensity from aluminum oxide and aluminum metal, from which film thickness can be estimated using the Hill Equation.[60]

The mathematics of optimization suggests that making use of lineshapes that best approximate photoemission shapes within a peak model is important to chemical state determination. Using lineshapes closest to observed peak shapes reduces the need to enforce parameter constraints during optimization, bearing in mind that the application of parameter constraints represents an input of user bias to a peak model. A number of components and lineshapes are essential inputs to peak models, while parameter constraints should be considered nonessential inputs but required to compensate for imperfections in lineshapes, backgrounds, and issues with signal-to-noise. There is, therefore, just cause to investigate asymmetric lineshapes other than the traditional forms, particularly for situations where narrow components are involved, and instrumental artifacts have increased influence over observed peak shapes.

G. Uniqueness plot

In this section, the impact of FWHM on a peak model is considered. The data analysis in Fig. 18, performed using a so-called uniqueness plot,[61] shows that a range of plausible figure-of-merit values is obtained through optimization involving specific FWHM values for the Ga 3s component. The uniqueness plot demonstrates how one can select an informed, fixed FWHM parameter for Ga 3s for use in fitting curves to an individual spectrum as the only means of establishing a physically meaningful peak model.

Each peak model includes parameters for peak position, FWHM, and area. FWHM differs from position and area in the sense that FWHM depends upon instrumental energy resolution, data acquisition conditions, as well as on the chemical state of the sample. Ideally, the BE and relative area for the component peaks will be independent of the instrumental energy resolution. Furthermore, there is correlated information between the lineshape and FWHM in the sense that lineshape parameters chosen also alter FWHW for the curve being fitted using the FWHM fitting parameter. By making a uniqueness plot, one can assess how a particular fitting parameter changes the outcome of curve fitting. This technique is applied to the FWHM for the data and curves shown in Fig. 18.

Optimization of the peak model shown in Fig. 18 was performed using optimization parameters that were free to adjust within physically meaningful intervals. The standard constraint (discussed in Fig. 8) on the component areas of the S 2p doublet
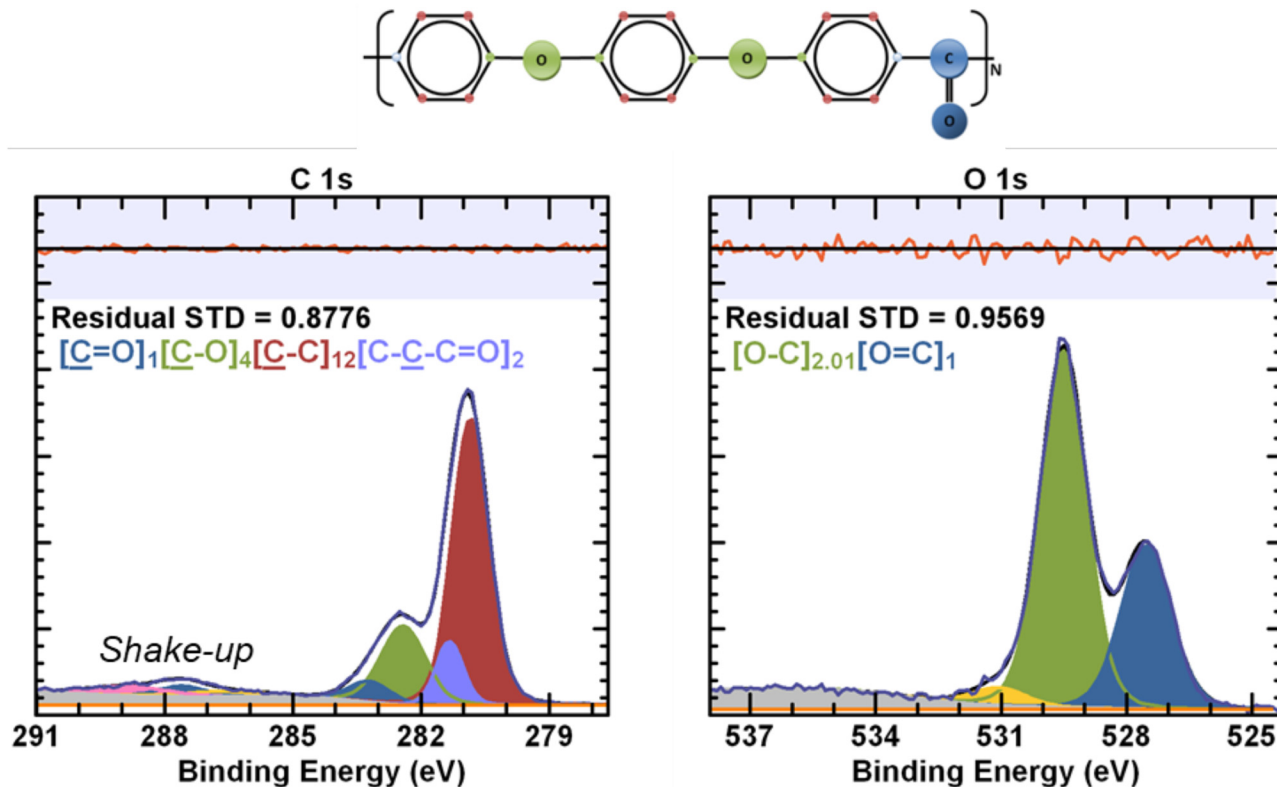
FIG. 13. High-resolution C 1s and O 1s spectra of PEEK. The colors of the peaks correspond to the colors of the carbon and oxygen atom types in the repeating PEEK polymer unit above. A background modeled the same was as in Figs. 11 and 12.

components was utilized in the original optimization model. One means of testing the influence of FWHM on a peak model is to specify a fixed FWHM value close to the value for the FWHM resulting from the original optimization, then refitting the new model to the same data. If repeated for a range of fixed FWHM values, a set of solutions with a new figure-of-merit result. The plot in Fig. 19 is that of a figure-of-merit plotted as a function of fixed FWHM values for the Ga 3s component in Fig. 18. The curve in Fig. 19 clearly shows a minimum in the figure-of-merit and significant deviation away from the minimum. The flatter this curve, the smaller the effect of the parameter on the fit. A flat curve in the uniqueness plot can often indicate that the peak that it belongs too is not appropriate for use in the peak model.

H. Curve-fitting data obtained with achromatic x rays

Lineshapes used in peak models are not necessarily transferable between data collected from different instruments. The most apparent differences occur for data collected using achromatic x-ray sources compared to monochromatic x-ray sources. XPS spectra collected with achromatic x rays are more complicated to fit due to the presence of an x-ray satellite structure. While many modern XPS instruments use monochromatic x rays, there are still
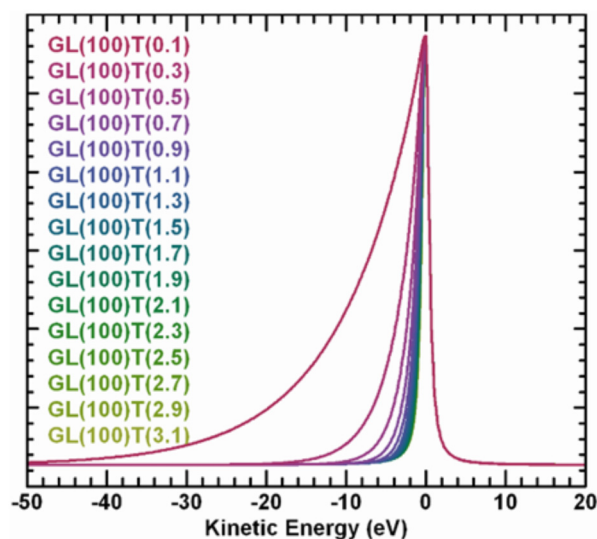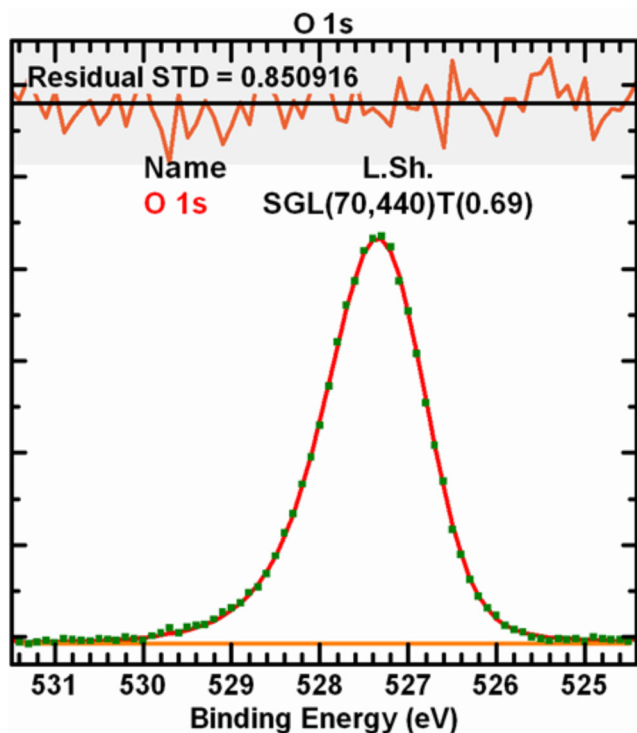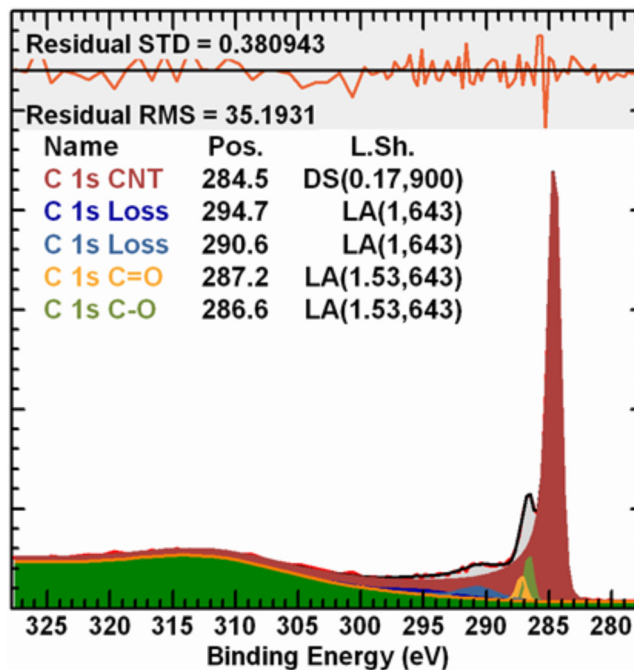

FIG. 14. Exponential tail lineshapes constructed using a Lorentzian profile modified by an exponential form as described in Beamson and Briggs (Ref. 36).

FIG. 15. O 1s signal from Nylon 6 modeled using an exponential tail modification to a Gaussian/Lorentzian SGL (70) symmetric lineshape (CASAXPS equivalent of GLS M = 0.7 lineshape as discussed above). The definitions of potential lineshapes are described in the Casa Software manual (Ref. 56). Following the formation of the exponential tail lineshape, the resulting asymmetric profile is further convoluted with a Gaussian. The assumption in using an asymmetric tail to model the O 1s measured from Nylon 6 is that the peak shape is a consequence of measurement conditions rather than additional chemistry due to contamination. The linear background was used.

FIG. 16. Multiwalled carbon nanotube C 1s data fitted making use of a Doniach–Sunjic lineshape (Ref. 28). The definitions of potential lineshapes are described in the Casa Software manual (Ref. 56). The peak model includes an example of an active approach to modeling the background signal. These data were acquired as a set of images using the imaging mode of an XPS instrument from which spectral data are processed. The residual standard deviation reflects adjustments to the raw pulse counted signal performed on images within the original data set. These data represent an example of data for which the target residual standard deviation is different from unity.

many instruments using achromatic x-ray sources. The energies of the x-ray satellites are well known, and to be effective, the curve fits need to include additional peaks for photoelectrons excited by these typically higher energy x rays.

In most cases, up to seven peaks can be included for each of the principal XPS peaks, these peaks corresponding to photoelectrons ejected by $K\alpha_{1,2}$, $K\alpha'$, $K\alpha_3$, $K\alpha_4$, $K\alpha_5$, $K\alpha_6$, K_β x rays. Since curve fitting is generally conducted over a narrow energy range (e.g., 10–25 eV), only the $K\alpha'$, $K\alpha_3$, $K\alpha_4$ x-ray satellites typically need to be included. Peaks excited by $K\alpha'$, $K\alpha_3$, $K\alpha_4$ x rays have intensities representing about 1%, 8%, and 6%, respectively, of the intensity of the main peak and are at 4.6, 8.4, and 10.2 eV lower BE than the principal peak. The other higher energy x-ray satellites need to be included when a wider energy range is fitted, for example, for a 50 eV range to cover the two spin–orbit split Ag 3d peaks.[62] Information for x-ray satellite energies and relative intensities can be obtained from x-ray emission spectra[29,63] or from XPS studies.[62]

I. Using complementary information from the valence band region to assist the interpretation of the core region

The valence band region provides complementary information to the core region since the appearance of the spectrum in this region is determined by the effect of chemical bonding and, in the case of many materials, especially metals, the extensive dispersion of the electron energy levels. This leads the valence band region to have a complex spectral shape where curve fitting is not as simply performed for the analysis of valence band as it is in core-level XPS. Overlays of the ground state density of states calculated using first-principles band structure theory,[64] or in suitable cases by cluster calculations, can be quite useful in interpreting valence band spectra. A study of the often complex shape of the valence band region can assist identification since it is the pattern that is characteristic of the material so that errors in calibration and thus BEs are less of an impediment to the correct interpretation of the data than they are in the core region. In other words, the valence band region can be a useful "fingerprint" for identifying materials.[65] Listed below are some examples where the valence band
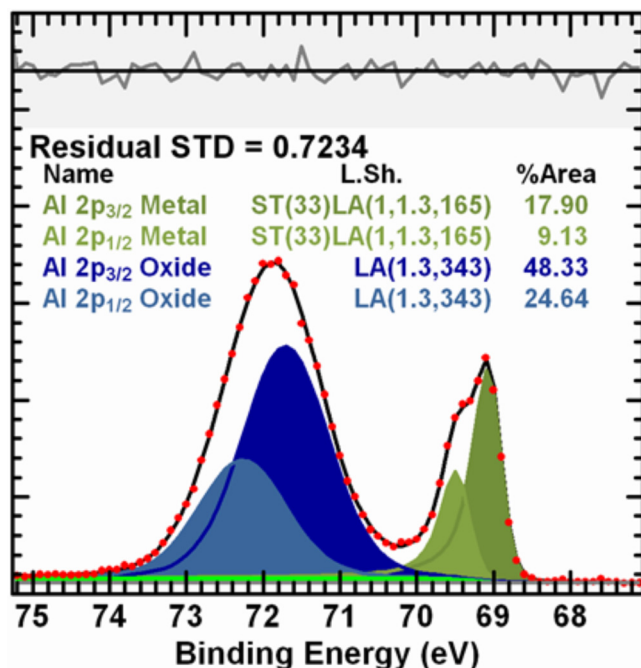
FIG. 17. Al 2p spectrum measured by John Walton (University of Manchester) from an aluminum foil. An asymmetric lineshape is applied to the narrow aluminum metal 2p doublet components while the oxide components are generalized Voigt functions. (Ref. 54) The definition of lineshapes is described in Casa Software manual (Ref. 56). A Shirley background is computed using the metal components, which only allows a flat background beneath the aluminum oxide components. Note how both the aluminum oxide and aluminum metal signals interact with each other via Lorentzianlike tails to these lineshapes.
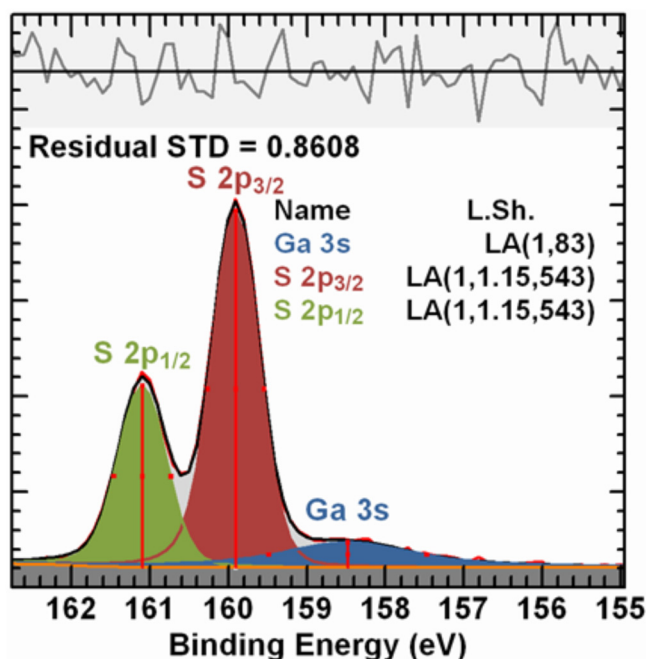
FIG. 18. A material including sulfur and gallium results in spectra with overlapping component peaks for S 2p and Ga 3s. These component peaks are examples of photoemission with significantly different lineshapes and significantly different FWHM fitting parameter values. The definition of lineshapes is described in the Casa Software manual (Ref. 56). Four-parameter universal cross section Tougaard background is used.

region can be especially effective in the identification of different chemical species, where this is particularly true when monochromatic X-radiation is used:

- Metals often have very distinct features in the valence band region, for example:
  o Molybdenum metal has a distinct four feature pattern at BEs below 5 eV, which can be explained by the calculated spectrum.[21,66]
- Silver metal has a distinct four feature pattern at BEs below 8 eV, which can be explained by the calculated spectrum.[21]
- Oxides often have distinct valence band features, including a multiple peak pattern in cases where the core region exhibits one peak with little or no BE shift between different oxidation states, for example:
  o Molybdenum oxides have distinctly different valence band spectra.[21,67]
  o Aluminum oxides and oxyhydroxides cannot reliably be distinguished in the Al 2p core region but show substantial differences in the valence band region.[64,68]
- Molecular ions such as sulfates, carbonates, and phosphates have distinguishable valence band features, for example:

  o Carbonates and bicarbonates can be distinguished.[69]
  o Different types of phosphates show no difference in the P 2p core region, but substantial differences in the valence band region (Fig. 20).[70,71]
- Polymers typically give a valence band that is rich in features. Thus, organic polymers with little or no difference in the C 1s region often show a valence band with very characteristic features.[36]

J. Reporting of fitting process and parameters

To enable others to understand and assess the results obtained from fitting of spectra, it is necessary that both the results and information about the fitting approach, constraints, and assumptions and final fitting parameters be included in journal articles or reports. ISO Standard 19830 describes the minimum reporting requirements for peak fitting in XPS.[72] Important parameters include spectrometer and x-ray characteristics, the use of charge compensation and charge correction, the type of spectral pre-preprocessing such as satellite subtraction, smoothing, and deconvolution, the type of background used, fitting parameters such as lineshapes, FWHM, and χ^2, as well as the software used for curve fitting.
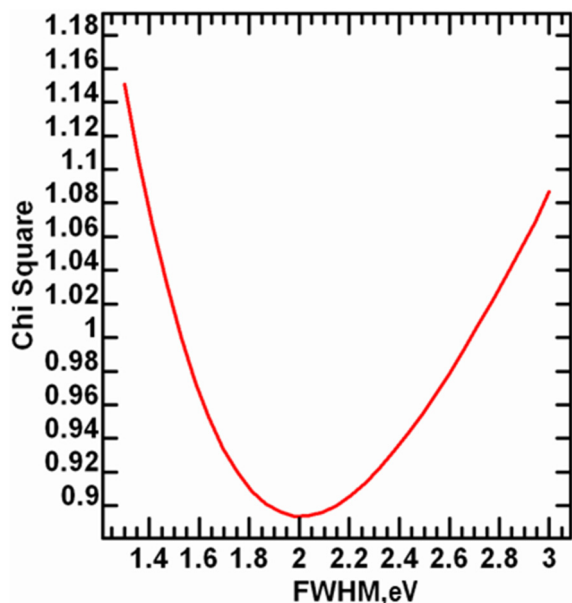
FIG. 19. Uniqueness plot based on scanning the Ga 3s FWHM for a range of fixed values in an interval of 1.3–3.0 eV. The FWHM achieved by optimization for the model in Fig. 18 is 2.0 eV. Note the figure-of-merit is within the range for all FWHM that would be acceptable as an indication of good data reproduction by a peak model, but the best value is clearly observable in the uniqueness plot.
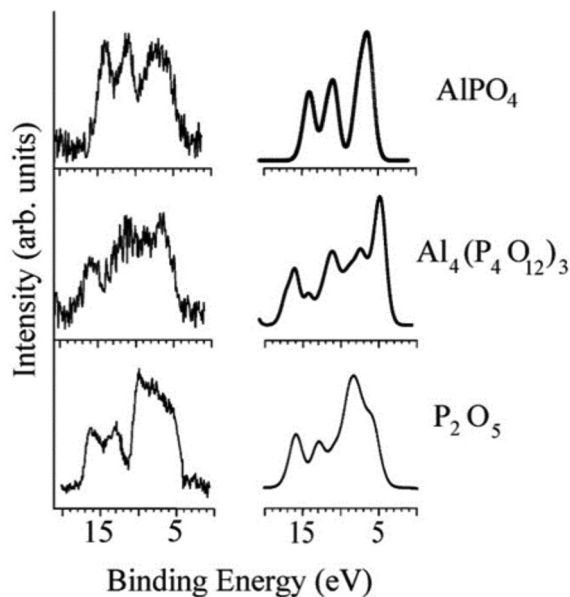

FIG. 20. Valence Band spectra of phosphorus-oxygen compounds. The experimental spectra are compared with spectra calculated from band structure calculations. A simple phosphate, $AlPO_4$, a ring phosphate $Al_4(P_4O_{12})_3$, and a three-dimensional P/O cluster (P_2O_5) are shown.

For the full list of minimum reporting parameters, please refer to ISO,[72] while here we include some of the recommended parameters. On the experimental side, the photon energy and the type of source (monochromatic or achromatic) should be listed. The type of analyzer and the geometry of the measurement should be described, including the expected resolution of the measurement. Finally, the form of the sample (solid, thin-film, powder) should be given. On the fitting side, the fitting parameters should be given in detail, including a description of the backgrounds used in the fit. Lineshapes and linewidths should be documented. If linewidths used vary significantly across a spectral fit, an explanation of why this is physically reasonable should be included. The software used in the analysis should be listed. Spectra should have a complete core level spectral range to include background and spin–orbit components. Tables of parameters, including error bars, will make the fitting information more accessible to the reader.

VII. SUMMARY AND CONCLUSIONS

As the use of XPS data in many areas of science and technology has become increasingly important, and the complexity of advanced materials has increased, the extraction of important physicochemical information increasingly requires the fitting of XPS data. Unfortunately, the processes used and the information obtained are often incorrect or incomplete,[3] and information associated with fitting processes and results is often not adequately reported. The good practices and information presented in this guide are provided as a guide to improving the quality of the XPS curve fitting reported in the literature.

One of the main objectives of the curve fitting of XPS data is to extract chemical information about the sample being examined. Consequently, curve fitting needs to be done in a manner that is consistent with the physics and chemistry of both the XPS process and the specimen being examined. It is also important to remember that the quality of chemical information extracted depends on the quality of data acquisition and data processing.

Many errors related to fitting and peak identification in the literature arise from authors not recognizing the impacts of not only intrinsic but also extrinsic phenomena, such as spin–orbit splitting or the effects of plasmons, multiplet splitting, or shake-up processes. The XPS peak positions and lineshapes are significantly affected by these processes. Such effects highlight the importance of relevant reference spectra in the understanding and fitting of peak structures.

In the application of curve fitting to XPS spectra, reference materials, consistency of approach to both reference and target materials, paying attention to the physics and chemistry of the photoelectron peaks, and appropriate reporting of the approach, software used, and fitting parameters are all critical. This guide has provided a summary of important issues and described tools and strategies that represent good practices important to useful, informative, and reproducible peak fitting of core-level XPS spectra.

REFERENCES

[1]C. J. Powell, Microsc. Today **24**, 16 (2016).
[2]P. M. A. Sherwood, Surf. Interface Anal. **51**, 589 (2019).
[3]M. R. Linford et al., Microsc. Microanal. **26**, 1 (2020).

[4]D. R. Baer and A. G. Shard, J. Vac. Sci. Technol. A **38**, 031203 (2020).

[5]D. Briggs and J. T. Grant, *Surface Analysis by Auger and X-Ray Photoelectron Spectroscopy* (IM Publications, Chichester, UK, 2003).

[6]V. Gupta, H. Ganegoda, M. H. Engelhard, J. Terry, and M. R. Linford, J. Chem. Educ. **91**, 232 (2014).

[7]G. H. Major *et al.*, "Perspective: An assessment of the frequency and nature of erroneous XPS analyses in the literature," Appl. Surf. Sci. (submitted).

[8]M. H. Engelhard, A. H. Gomez, P. M. A. Sherwood, and D. R. Baer, J. Vac. Sci. Technol. A **38**, 063203 (2020).

[9]T. Deegan, "X-ray photoelectron spectrometer calibration and thin film investigations on germanium oxides," Master of science thesis (Dublin City University, 1998).

[10]J. F. Moulder, *Handbook of X-ray Photoelectron Spectroscopy: A Reference Book of Standard Spectra for Identification and Interpretation of XPS Data* (Physical Electronics, Eden Prairie, MN, 1992).

[11]ISO 16129:2018, *X-ray Photoelectron Spectroscopy—Procedures for Assessing the Day-to-Day Performance of an X-ray Photoelectron Spectrometer* (International Organization for Standardization, Geneva, 2018).

[12]ASTM E2735-14, ASTM International, West Conshohocken, PA (2014).

[13]J. Wolstenholme, J. Vac. Sci. Technol. A **38**, 043206 (2020).

[14]R. Bracewell, *The Fourier Transform and Its Applications*, 3rd ed. (McGraw-Hill Science/Engineering/Math, New York, 1999).

[15]G. Major, T. Avval, N. Fairley, and M. Linford, Vac. Technol. Coat. **21**, 37 (2020), available at https://digital.vtcmag.com/12727/26337/index.html.

[16]D. R. Baer *et al.*, J. Vac. Sci. Technol. A **38**, 031204 (2020).

[17]A. Einstein, Ann. Phys. **322**, 132 (1905).

[18]P. H. Citrin and D. R. Hamann, Phys. Rev. B **15**, 2923 (1977).

[19]W. Voigt, Akad. Wiss. München, Math. Phys. **216**, 603 (1912).

[20]V. Jain, M. C. Biesinger, and M. R. Linford, Appl. Surf. Sci. **447**, 548 (2018).

[21]P. M. A. Sherwood, Surf. Interface Anal. **51**, 254 (2019).

[22]J. C. Fuggle and S. F. Alvarado, Phys. Rev. A **22**, 1615 (1980).

[23]M. O. Krause and J. H. Oliver, J. Phys. Chem. Ref. Data **8**, 329 (1979).

[24]P. L. Lee and S. I. Salem, Phys. Rev. A **10**, 2027 (1974); R. C. Rivière, *Practical Surface Analysis*, edited by D. Briggs and M. P. Seah (Wiley, Chichester, UK, 1990), pp. 75–83.

[25]D. Roy and D. Tremblay, Rep. Prog. Phys. **53**, 1621 (1990); P. M. A. Sherwood, *Vibrational Spectroscopy of Solids* (Cambridge University, Cambridge, 1972).

[26]C. N. Berglund and W. E. Spicer, Phys. Rev. A **136**, 1030 (1964).

[27]A. Barrie, Chem. Phys. Lett. **19**, 109 (1973).

[28]S. Doniach and M. Sunjic, J. Phys. C Solid State **3**, 285 (1970).

[29]T. A. Carson, *Photoelectron and Auger Spectroscopy,* Modern Analytical Chemistry (Springer, Boston, MA, 1975).

[30]A. Herrera-Gomez, M. Bravo-Sanchez, O. Ceballos-Sanchez, and M. O. Vazquez-Lepe, Surf. Interface Anal. **46**, 897 (2014).

[31]D. I. Patel, S. Bahr, P. Dietrich, M. Meyer, A. Thißen, and M. R. Linford, Surf. Sci. Spectra **26**, 014024 (2019).

[32]D. Shah, S. Bahr, P. Dietrich, M. Meyer, A. Thißen, and M. R. Linford, Surf. Sci. Spectra **26**, 014023 (2019).

[33]M. Salmeron and R. Schlögl, Surf. Sci. Rep. **63**, 169 (2008).

[34]K. Roy, L. Artiglia, and J. A. van Bokhoven, Chem. Cat. Chem. **10**, 666 (2018).

[35]A. Shard, J. Vac. Sci. Technol. A **38**, 041201 (2020).

[36]G. Beamson and D. Briggs, *High Resolution XPS of Organic Polymers: The Scienta ESCA300 Database* (Wiley, Chichester, 1992).

[37]C. D. Easton, C. Kinnear, S. L. McArthur, and T. R. Gengenbach, J. Vac. Sci. Technol. A **38**, 023207 (2020).

[38]G. Greczynski and L. Hultman, Prog. Mater. Sci. **107**, 100591 (2020).

[39]MultPak 9.9, Ulvac-phi (1994–2016).

[40]NIST X-ray Photoelectron Spectroscopy Database, NIST Standard Reference Database Number 20 (National Institute of Standards and Technology, Gaithersburg MD, 2000), https://srdata.nist.gov/xps/.

[41]See http://techdb.podzone.net/eindex.html for XPS (X-ray Photoelectron Spectroscopy) Database.

[42]M. C. Biesinger, see http://www.xpsfitting.com/ for X-ray Photoelectron Spectroscopy (XPS) Reference Page (2009–2018).

[43]XPS Reference Table of Elements, Thermo Fisher Scientific (2013–2020).

[44]XPS Reference Table of Elements, Scientific™.

[45]eSpectra visualization too, AIP Publishing LLC.

[46]A. J. Barlow, R. T. Jones, A. J. McDonald, and P. J. Pigram, Surf. Interface Anal. **50**, 527 (2018).

[47]M. C. Biesinger, B. P. Payne, L. W. M. Lau, A. Gerson, and R. S. C. Smart, Surf. Interface Anal. **41**, 324 (2009).

[48]M. C. Biesinger, B. P. Payne, A. P. Grosvenor, L. W. M. Lau, A. R. Gerson, and R. S. C. Smart, Appl. Surf. Sci. **257**, 2717 (2011).

[49]M. C. Biesinger, L. W. M. Lau, A. R. Gerson, and R. S. C. Smart, Appl. Surf. Sci. **257**, 887 (2010).

[50]R. Kramer, *Chemometric Techniques for Quantitative Analysis* (CRC Press, Boca Raton, FL, 1998).

[51]J. H. Scofield, J. Electron. Spectrosc. **8**, 129 (1976).

[52]N. Mårtensson and R. Nyholm, Phys. Rev. B **24**, 7121 (1981).

[53]D. O. Scanlon, G. W. Watson, D. J. Payne, G. R. Atkinson, R. G. Egdell, and D. S. L. Law, J. Phys. Chem. C **114**, 4636 (2010).

[54]G. Major, D. Shah, V. Fernandez, N. Fairley, and M. Linford, Vac. Technol. Coat. **21**, 43 (2020), available at https://digital.vtcmag.com/12727/29865/index.html.

[55]G. Major, D. Shah, T. Avval, V. Fernandez, N. Fairley, and M. Linford, Vac. Technol. Coat. **21**, 35 (2020), available at https://digital.vtcmag.com/12727/26337/index.html.

[56]CasaXPS, Casa Software Ltd (2020).

[57]E. Desimoni, G. I. Casella, T. R. I. Cataldi, and C. Malitesta, J. Electron. Spectrosc. **49**, 247 (1989).

[58]M. Schmid, H.-P. Steinrück, and J. M. Gottfried, Surf. Interface Anal. **46**, 505 (2014).

[59]M. Bravo Sanchez, J. A. Huerta-Ruelas, D. Cabrera-German, and A. Herrera-Gomez, Surf. Interface Anal. **49**, 253 (2017).

[60]J. M. Hill, D. G. Royce, C. S. Fadley, L. F. Wagner, and F. J. Grunthaner, Chem. Phys. Lett. **44**, 225 (1976).

[61]B. Singh, A. Diwan, V. Jain, A. Herrera-Gomez, J. Terry, and M. R. Linford, Appl. Surf. Sci. **387**, 155 (2016).

[62]P. M. A. Sherwood, J. Vac. Sci. Technol. A **14**, 1424 (1996).

[63]M. O. Krause and J. G. Ferreira, J. Phys. B At. Mol. Opt. **8**, 2007 (1975).

[64]J. A. Rotole and P. M. A. Sherwood, J. Vac. Sci. Technol. A **17**, 1091 (1999).

[65]D. S. Jensen *et al.*, Surf. Interface Anal. **45**, 1273 (2013).

[66]P. M. A. Sherwood, *Practical Surface Analysis by Auger and X-ray Photoelectron Spectroscopy*, edited by D. Briggs and M. P. Seah (Wiley, New York, 1983).

[67]H. Hixson and P. M. A. Sherwood, Chem. Mater. **8**, 2643 (1996).

[68]S. Thomas and P. M. A. Sherwood, Anal. Chem. **64**, 2488 (1992).

[69]S. Thomas and P. M. A. Sherwood, Surf. Interface Anal. **20**, 595 (1993).

[70]P. M. A. Sherwood, Surf. Sci. Spectra **9**, 62 (2002).

[71]K. J. Gaskell, M. M. Smith, and P. M. A. Sherwood, J. Vac. Sci. Technol. A **22**, 1331 (2004).

[72]ISO 19830:2015, *Electron Spectroscopies—Minimum Reporting Requirements for Peak Fitting in X-ray Photoelectron Spectroscopy* (International Organization for Standardization, Geneva, 2015).